



1

2

3

4

5

6

7 **Air quality and health benefits from ultra-low emission**

8 **control policy indicated by continuous emission monitoring:**

9 **A case study in the Yangtze River Delta region, China**

10

11 Yan Zhang<sup>1</sup>, Yu Zhao<sup>1,2\*</sup>, Meng Gao<sup>3</sup>, Xin Bo<sup>4</sup>, Chris P. Nielsen<sup>5</sup>

12

13 1. State Key Laboratory of Pollution Control and Resource Reuse and School of the  
14 Environment, Nanjing University, 163 Xian in Ave., Nanjing, Jiangsu 210023, China.

15 2. Jiangsu Collaborative Innovation Center of Atmospheric Environment and  
16 Equipment Technology (CICAEET), Nanjing University of Information Science and  
17 Technology, Jiangsu 210044, China.

18 3. Department of Geography, State Key Laboratory of Environmental and Biological  
19 Analysis, Hong Kong Baptist University, Hong Kong SAR, China.

20 4. The Appraisal Center for Environment and Engineering, Ministry of Environmental  
21 Protection, Beijing 100012, China.

22 5. Harvard-China Project on Energy, Economy and Environment, John A. Paulson  
23 School of Engineering and Applied Sciences, Harvard University, 29 Oxford St,  
24 Cambridge, MA 02138, USA.

25

26

27 \*Corresponding author: Yu Zhao

28 Phone: 86-25-89680650; email: [yuzhao@nju.edu.cn](mailto:yuzhao@nju.edu.cn)

29



## 30 Abstract

31 To evaluate improved emission estimation from online monitoring data, we  
32 applied the Models-3/CMAQ (Community Multi-scale Air Quality) system to  
33 simulate the air quality of the Yangtze River Delta (YRD) region using two emission  
34 inventories without/with incorporated data from continuous emission monitoring  
35 systems (CEMS) at coal-fired power plants (Cases 1 and 2), respectively. The  
36 normalized mean biases (NMBs) of annual SO<sub>2</sub>, NO<sub>2</sub>, O<sub>3</sub> and PM<sub>2.5</sub> concentrations  
37 between observations and simulations in Case 2 were -3.1%, 56.3%, -19.5% and  
38 -1.4%, all smaller in absolute value than those in Case 1, at 8.2%, 68.9%, -24.6% and  
39 7.6%, respectively. The results indicate that incorporation of CEMS data in the  
40 emission inventory helped reduce the biases between simulation and observation and  
41 can better reflect the actual sources of regional air pollution. Based on the CEMS data,  
42 the air quality changes and corresponding health impacts were quantified for different  
43 implementation levels of China's recent "ultra-low" emission policy. If only the  
44 coal-fired power sector met the requirement, the simulated differences in the monthly  
45 SO<sub>2</sub>, NO<sub>2</sub>, O<sub>3</sub> and PM<sub>2.5</sub> concentrations compared to those of Case 2, our base case for  
46 policy comparisons, were less than 7% for all pollutants. The result implies only a  
47 minor benefit of ultra-low emission control if implemented in the power sector alone,  
48 attributed to its limited contribution to total emissions in the YRD after years of  
49 pollution control in the sector (11%, 7% and 2% of SO<sub>2</sub>, NO<sub>x</sub> and primary particle  
50 matter (PM), respectively). If the ultra-low emission policy was enacted at both power  
51 plant and industrial boilers, the simulated SO<sub>2</sub>, NO<sub>2</sub> and PM<sub>2.5</sub> concentrations  
52 compared to the base case were 33%-64%, 16%-23% and 6%-22% lower respectively,  
53 depending on the month (January, April, July and October 2015). Combining CMAQ  
54 and the Integrated Exposure Response (IER) model, we further estimated that 305  
55 deaths and 874 years of life loss (YLL) attributable to PM<sub>2.5</sub> exposure could be  
56 avoided with the implementation of the ultra-low emission policy in the power sector  
57 in the YRD region. The analogous values would be much higher, at 10,651 deaths and  
58 316,562 YLL avoided, if both power and industrial sectors met the ultra-low emission  
59 limits, accounting for 5.5% and 6.2% of the totals for the region, respectively. In order  
60 to improve regional air quality and to reduce human health risk effectively,  
61 coordinated control of various pollution sources should be implemented, and the



62 ultra-low emission control policy should be substantially expanded to industrial  
63 boilers and other emission sources in non-power industries.

## 64 1. Introduction

65 Due to swift economic development and associated growth in demand for  
66 electricity, coal-fired power plants have played an important role in energy  
67 consumption and air pollutant emissions for a long time in China. For example, Zhao  
68 et al. (2008) for the first time developed a “unit-based” emission inventory of primary  
69 air pollutants from the coal-fired power sector in China and found that the sector  
70 contributed 53% and 36% to the national total emissions of SO<sub>2</sub> and NO<sub>x</sub>,  
71 respectively, in 2005. Subsequently, SO<sub>2</sub> and NO<sub>x</sub> emissions from the power sector  
72 were estimated to account respectively for 28%-53% and 29%-31% of the total annual  
73 emissions in China during 2006-2010 according to the Multi-resolution Emission  
74 Inventory for China (MEIC: <http://www.meicmodel.org>). To reduce high emissions  
75 and improve air quality in China, advanced air pollutant control devices (APCDs)  
76 have been gradually applied in the power sector including flue gas desulfurization  
77 (FGD) for SO<sub>2</sub> control, selective catalytic reduction (SCR) for NO<sub>x</sub> control, and  
78 high-efficiency dust collectors for primary particulate matter (PM) control. In recent  
79 years, moreover, an “ultra-low emission” retrofitting policy has been widely  
80 implemented, seeking to reduce the emission levels of coal-fired power plants to those  
81 of gas-fired ones (i.e., 35, 50, and 5 mg/m<sup>3</sup> for SO<sub>2</sub>, NO<sub>x</sub> and PM concentrations in  
82 the flue gas). The expanded use of associated technologies has induced great changes  
83 in the magnitude and spatio-temporal distribution of emissions from the power sector,  
84 which have been analyzed and quantified by a series of studies (Y. Zhao et al., 2013;  
85 Zhang et al., 2018; Liu et al., 2019; Tang et al., 2019; Y. Zhang et al., 2019). With the  
86 updated unit-level information, for example, MEIC estimated that the power sector  
87 shares of national total emissions declined from 28% to 22% and from 29% to 21%  
88 for SO<sub>2</sub> and NO<sub>x</sub> during 2010-2015, respectively. Incorporating data from continuous  
89 emission monitoring systems (CEMS), Tang et al. (2019) found that China’s annual  
90 power sector emissions of SO<sub>2</sub>, NO<sub>x</sub> and PM declined by 65%, 60% and 72%  
91 respectively during 2014-2017, due to the enhanced control measures. With a method  
92 of collecting, examining and applying CEMS data, similarly, our previous work  
93 indicated that the estimated emissions from the power sector would be 75%, 63% and



94 76% smaller than those calculated without CEMS data for SO<sub>2</sub>, NO<sub>x</sub> and PM,  
95 respectively (Y. Zhang et al., 2019).

96 Evaluations of emission estimates and the changed air quality from emission  
97 abatement provide useful information on the sources of air pollution and the  
98 effectiveness of pollution control measures. Air quality modeling is an important tool  
99 for evaluating emission inventories, by comparing simulation results with available  
100 observation data. Developed by the U.S. Environmental Protection Agency (USEPA),  
101 the Models-3/Community Multi-scale Air Quality (CMAQ) system has been widely  
102 used in China (Li et al., 2012; An et al., 2013; Wang et al., 2014; Han et al., 2015;  
103 Zheng et al., 2017; Zhou et al., 2017; Chang et al., 2019). Han et al. (2015) conducted  
104 CMAQ simulations with different emission inventories for East Asia, and found that  
105 the simulated NO<sub>2</sub> columns using the emission inventory for the Intercontinental  
106 Chemical Transport Experiment-Phase B (INTEX-B, Zhang et al., 2009) agreed better  
107 with the satellite observations of the Ozone Monitoring Instrument (OMI) than the  
108 simulations using the Regional Emission Inventory in Asia (REAS v1.11, Ohara et al.,  
109 2007). Zhou et al. (2017) applied CMAQ to evaluate the national, regional and  
110 provincial emission inventories for the Yangtze River Delta (YRD) region, and the  
111 best model performance with the provincial inventory confirmed that the emission  
112 estimate with more detailed information incorporated on individual power and  
113 industrial plants helped improve the air quality simulation at relatively high horizontal  
114 resolution. With air quality modeling, moreover, many studies have explored the  
115 environment benefits of emission control measures taken in recent years (B. Zhao et  
116 al., 2013; Huang et al., 2014; Li et al., 2015; Wang et al., 2015; Tan et al., 2017).  
117 Wang et al. (2015) found that the implementation of the new Emission Standard of Air  
118 Pollutants for Thermal Power Plants (GB13223-2011) could effectively reduce  
119 pollutant emissions in China, and the environmental concentrations of SO<sub>2</sub>, NO<sub>2</sub> and  
120 PM<sub>2.5</sub> would decrease by 31.6%, 24.3% and 14.7% respectively in 2020 compared  
121 with a baseline scenario for 2010. Li et al. (2015) found that the simulated  
122 concentrations of PM<sub>2.5</sub> in the YRD region would decrease by 8.7%, 15.9% and 24.3%  
123 from 2013 to 2017 in three scenarios with weak, moderate and strong emission  
124 reduction assumptions in the Clean Air Action Plan, respectively.

125 Besides air quality itself, the health risk caused by air pollution exposures in  
126 China is a major concern, especially to PM<sub>2.5</sub>, a dominant pollutant in haze conditions.



127 Lim et al. (2012) has identified air pollution as a primary cause of global burden of  
128 disease, especially in low- and middle-income countries, and PM<sub>2.5</sub> pollution was  
129 ranked the fourth leading cause of death in China. Studies have shown that PM<sub>2.5</sub> is  
130 closely related to several causes of death (Dockery et al., 1993; Hoek et al., 2013;  
131 Lelieveld et al., 2015; Butt et al., 2017; Gao et al., 2018; Maji et al., 2018; Hong et al.,  
132 2019). For example, Lelieveld et al. (2015) estimated that nearly 1.4 million people  
133 died each year due to PM<sub>2.5</sub> exposure in China, 18% of which were related to the  
134 emissions from the power sector. Based on simulated PM<sub>2.5</sub> using WRF-Chem and the  
135 Integrated Exposure Response (IER) model, Gao et al. (2018) estimated that  
136 emissions from the power sector results in 15 million years of life lost per year in  
137 China. In addition to assessment of health risk based on observations of actual air  
138 pollution levels, studies have also analyzed the health benefits of emission control  
139 policies (Lei et al., 2015; Li and Li, 2018; Dai et al., 2019; Q. Zhang et al., 2019; X.  
140 Zhang et al., 2019). Combining available observation and CMAQ modeling, Q. Zhang  
141 et al. (2019) identified improved emission controls on industrial and residential  
142 pollution sources as the main drivers of reductions in PM<sub>2.5</sub> concentrations from 2013  
143 to 2017 in China, and estimated an annual reduction of PM<sub>2.5</sub>-related deaths at 0.41  
144 million. Lei et al. (2015) evaluated the health benefit of the Air Pollution Prevention  
145 and Control Action Plan of China, and found that full realization of the air quality  
146 goal in this plan could avoid 89 thousand premature deaths of urban residents, and  
147 reduce 120,000 inpatient cases and 9.4 million outpatient service and emergency cases.  
148 Focusing more regionally, X. Zhang et al. (2019) estimated the health impact of a  
149 "coal-to-electricity" policy for residential energy use in the Beijing-Tianjin-Hebei  
150 (BTH) region. They projected that the reduction in PM<sub>2.5</sub> concentrations from the  
151 policy would avoid nearly 22,200 cases of premature death and 607,800 cases of  
152 disease in the region in 2020. For areas with strong, industry-based economies, the  
153 impact of air quality on public health can be more significant, attributed both to  
154 relatively large and dense populations and to high pollution levels. Until now,  
155 however, there have been few studies focusing on air quality improvement and  
156 corresponding health benefits attributed to the implementation of the latest emission  
157 control policies, notably China's ultra-low emission policy introduced above, at  
158 regional scale.

159 As one of the most densely populated and economically developed regions, the



160 YRD region encompassing Shanghai and Anhui, Jiangsu, and Zhejiang provinces is a  
161 key area for air pollution prevention and control in China (Huang et al., 2011; Li et al.,  
162 2011; Li et al., 2012). It is also one of the regions with the earliest implementation of  
163 the ultra-low emission policy on the power sector in the country. Quantification of  
164 emission reductions and subsequent changes in air quality is crucial for full  
165 understanding of the environmental benefits of the policy. To test the possible  
166 improvement in the regional emission inventory, this study evaluated the air quality  
167 modeling performance without and with CEMS data incorporated in the estimation of  
168 emissions of the coal-fired power sector for the YRD region. The changes in regional  
169 air quality and health risk resulting from the implementation of the ultra-low emission  
170 policy for key industries were quantified combining the air quality modeling and the  
171 health risk model. The results provide scientific support for incorporation of online  
172 monitoring data to improve the estimation of air pollutant emissions, and for better  
173 design of emission control policies based on their simulated environmental effects.  
174

## 175 **2. Methodology and data**

### 176 **2.1 Air quality modeling**

177 In this study, we adopted CMAQ version 4.7.1 (UNC, 2010) to conduct air  
178 quality simulations and to evaluate various emission inventories for the YRD region.  
179 The model has performed well in Asia (Zhang et al., 2006; Uno et al., 2007; Fu et al.,  
180 2008; Wang et al., 2009). Two one-way nested domains were adopted for the  
181 simulations, and the horizontal resolutions were set at 27 and 9 km square grid cells  
182 respectively, as shown in Figure 1. The mother domain (D1,  $177 \times 127$  cells) covered  
183 most of China and all or parts of surrounding countries in East, Southeast, and South  
184 Asia. The second modeling region (D2,  $118 \times 121$  cells) covered the YRD region,  
185 including Jiangsu, Zhejiang, Shanghai, Anhui and parts of surrounding provinces.  
186 Lambert Conformal Conic Projection was applied for the entire simulation area  
187 centered at ( $110^\circ\text{E}$ ,  $34^\circ\text{N}$ ) with two true latitudes,  $40^\circ\text{N}$  and  $25^\circ\text{N}$ . The simulated  
188 periods were January, April, July and October 2015, as representative of the four  
189 seasons. The first five days in each month were set as a spin-up period to provide  
190 initial conditions for later simulations. The carbon bond gas-phase mechanism (CB05)



191 and AERO5 aerosol module were adopted in all the CMAQ modules, with details of  
192 the model configuration found in Zhou et al. (2017). The initial concentrations and  
193 boundary conditions for the D1 mother domain were the default clean profile, while  
194 they were extracted from CMAQ outputs of D1 simulations for the nested D2 domain.  
195 Normalized mean bias (NMB), normalized mean error (NME), and the correlation  
196 coefficient (R) between the simulations and observations were selected to evaluate the  
197 performance of CMAQ modeling (Yu et al., 2006). The hourly concentrations of SO<sub>2</sub>,  
198 NO<sub>2</sub>, O<sub>3</sub> and PM<sub>2.5</sub> were observed at 230 state-operated ground stations of the national  
199 monitoring network in the YRD region and were collected from Qingyue Open  
200 Environmental Data Center (<https://data.epmap.org>).

201 The Weather Research and Forecasting (WRF) Model version 3.4  
202 (<http://www.wrf-model.org/index.php>, Skamarock et al., 2008) was applied to provide  
203 meteorological fields for CMAQ. Terrain and land-use data were taken from global  
204 data of the U.S. Geological Survey (USGS), and the first-guess fields of  
205 meteorological modeling were obtained from the final operational global analysis data  
206 (ds083.2) by the National Center for Environmental Prediction (NCEP). Statistical  
207 indicators including bias, index of agreement (IOA), and root mean squared error  
208 (RMSE) were chosen to evaluate the performance of WRF modeling against  
209 observations (Baker et al., 2004; Zhang et al., 2006). Ground observations at 3-h  
210 intervals of four meteorological parameters including temperature at 2 m (T2),  
211 relative humidity at 2 m (RH2), and wind speed and direction at 10 m (WS10 and  
212 WD10) of 42 surface meteorological stations in the YRD region were downloaded  
213 from the National Climatic Data Center (NCDC). The statistical indicators for WS10,  
214 WD10, T2 and RH2 in the YRD region are summarized by month in Table S1 in the  
215 Supplement. The discrepancies between WRF simulations and observations of these  
216 meteorological parameters were generally acceptable (Emery et al., 2001). Better  
217 agreements were found for T2 and RH2 with their biases ranging -0.62 to +0.12°C  
218 and -3.20% to +6.60% respectively, and their IOAs were all within the benchmarks  
219 (Emery et al., 2001). In general, WRF captured well the characteristics of main  
220 meteorological conditions for the region.

## 221 **2.2 Emission inventories and cases**

222 The anthropogenic emissions from industry, residential and transportation sectors



223 for D1 and D2 were obtained from the national emission inventory developed in our  
224 previous work (Xia et al., 2016). The total emissions excluding those of the power  
225 sector of SO<sub>2</sub>, NO<sub>x</sub> and PM for the YRD regions were estimated at 1501.0, 3468.4  
226 and 2711.2 Gg for 2015, respectively. The emission inventory in Xia et al. (2016) was  
227 developed using activity data at the provincial level, and the spatial distribution of  
228 emissions by sector was conducted according to that of MEIC with the original spatial  
229 resolution of 0.25° × 0.25° in this study. The gridded emissions were further  
230 downscaled to horizontal resolutions of 27 and 9 km in D1 and D2, respectively,  
231 based on the spatial distribution of population (for residential sources), industrial  
232 gross domestic product (for industrial sources), and the road network (for on-road  
233 vehicles). The monthly variations of emissions from each sector were assumed to be  
234 the same as in MEIC. In addition, the Model Emissions of Gases and Aerosols from  
235 Nature developed under the Monitoring Atmospheric Composition and Climate  
236 project (MEGAN-MACC, Guenther et al., 2012; Sindelarova et al., 2014) were  
237 applied as the biogenic emission inventory, and the emissions of Cl, HCl and lightning  
238 NO<sub>x</sub> were obtained from the Global Emissions Initiative (GEIA, Price et al., 1997).

239 For the power sector in the YRD region specifically, we adopted the unit-level  
240 emission estimates from our previous study and allocated the emissions according to  
241 the actual locations of individual units (Y. Zhang et al., 2019). As described in the  
242 study, the detailed information at the power unit level was compiled based on official  
243 environmental statistics including the installed capacity, fossil fuel consumption,  
244 combustion technology, and APCDs. The geographic locations of power units were  
245 taken initially from the environmental statistics, and then adjusted using Google Earth.  
246 As shown in in Table 1, in total five emission cases were set for the air quality  
247 simulation. Cases 1 and 2 used estimates of power sector emissions without/with  
248 incorporation of CEMS data, and were compared against each other to evaluate the  
249 benefit of online emission monitoring information in air quality simulation. Note Case  
250 2 was set as the base case for further analysis of the effects of emission controls.  
251 Based on the unit-level information from CEMS, Cases 3 and 4 calculated emissions  
252 assuming that only power plant boilers, or both power plant and industrial boilers  
253 meet the requirements of the ultra-low emission policy, respectively. The model  
254 performances were compared with the base case to quantify the air quality  
255 improvements that result from the policy. Case 5 removed all the emissions from the



256 power sector and thus helped to specify the contribution of the power sector to air  
257 pollution in the YRD region.

258 The air pollutant emissions for all the cases are summarized by sector in Table S2  
259 in the Supplement. With the CEMS data for the power sector incorporated, the total  
260 emissions of SO<sub>2</sub>, NO<sub>x</sub> and PM for the YRD region in Case 2 were estimated as 427,  
261 618 and 331 Gg smaller than those in Case 1, with relative reductions of 20%, 14%  
262 and 11% respectively. Benefiting from the implementation of the ultra-low emission  
263 policy in the coal-fired power sector, the total emissions of anthropogenic SO<sub>2</sub>, NO<sub>x</sub>  
264 and PM in Case 3 would further decline 123, 135 and 36 Gg compared to Case 2,  
265 respectively. The analogous numbers for Case 4 were 1180, 1003, and 1315 Gg, and  
266 the reduction rates compared to Case 2 were 70%, 27%, and 48% for SO<sub>2</sub>, NO<sub>x</sub> and  
267 PM, respectively. The implementation of the ultra-low emission policy for both power  
268 and industry sectors would significantly reduce the primary pollutant emissions for  
269 the YRD region. In Case 5 where the emissions from power sector were set as zero,  
270 the total emissions of SO<sub>2</sub>, NO<sub>x</sub> and PM were estimated to decrease by 11%, 7% and  
271 2% respectively compared to Case 2.

### 272 2.3 Health effect analysis

273 We applied the IER model of the Global Burden of Disease Study (GBD) 2015  
274 (Cohen et al., 2017) and quantified the impact of emission control policy on the  
275 human health risk due to long-term exposure of PM<sub>2.5</sub> in the YRD region. The number  
276 of attributable deaths and years of life lost (YLL) caused by long-term PM<sub>2.5</sub> exposure  
277 for selected emission cases were calculated for five diseases in this study. It  
278 considered the four adult diseases of the GBD study, including ischemic heart disease  
279 (IHD), stroke (STK, including ischemic and hemorrhagic stroke), lung cancer (LC),  
280 and chronic obstructive pulmonary disease (COPD), and a common disease among  
281 young children, acute lower respiratory infection (LRI).

282 The health risks in the different emission cases were estimated following Gao et  
283 al. (2018) with the updated information for 2015. First, the relative risk (RR) for each  
284 disease was calculated using eq. (1):

$$285 \quad RR_{i,j,k}(Cl) = \begin{cases} 1 + \partial_{i,j,k}(1 - e^{-\beta_{i,j,k}(Cl-C_0)^{\gamma_{i,j,k}}}), & Cl \geq C_0 \\ 1, & Cl < C_0 \end{cases} \quad (1)$$



286 where  $i$ ,  $j$ , and  $k$  represent the age, gender and disease type, respectively;  $Cl$  is the  
287 annual average  $PM_{2.5}$  concentration simulated with WRF-CMAQ (the average of  
288 January, April, July and October in this work);  $C_0$  is the counterfactual concentration;  
289 and  $\partial$ ,  $\beta$  and  $\gamma$  are the parameters that describe the IER functions, as reported by  
290 Cohen et al. (2017).

291 Secondly, the population attributable fractions (PAF) were calculated with RR  
292 following eq. (2) by disease, age and gender subgroup:

$$293 \quad PAF_{i,j,k} = \frac{RR_{i,j,k}(Cl) - 1}{RR_{i,j,k}(Cl)} \quad (2)$$

294 Moreover, the mortality attributable to  $PM_{2.5}$  exposure ( $\Delta M$ ) was calculated  
295 using eq. (3), where  $y_0$  is the current age-gender-specific mortality rate, and  $Pop$   
296 represent the exposed population in the age-gender-specific group in grid cell  $l$ :

$$297 \quad \Delta M_{i,j,k,l} = PAF_{i,j,k,l} \times y_{0i,j,k,l} \times Pop_{i,j,l} \quad (3)$$

298 The population data of the four provinces and cities in the YRD region were  
299 obtained from statistical yearbooks (AHBS, 2016; JSBS, 2016; SHBS, 2016; ZJBS,  
300 2016), and the gender distribution is shown in Table S3 in the Supplement. The  
301 baseline age-gender-disease-specific mortality rates for the five diseases in China for  
302 2015 were obtained from the Global Health Data Exchange database (GHDx,  
303 <https://vizhub.healthdata.org>), as shown in Table S4 in the Supplement, and those by  
304 province were calculated based on the provincial proportions in Xie et al. (2016). The  
305 national population with the spatial resolution at  $1 \times 1$  km in 2015 was provided by the  
306 Landscan Global Demographic Dynamic Analysis Database developed by Oak Ridge  
307 National Laboratory (ORNL) of the U.S. Department of Energy. As shown in Figure  
308 S1 in the Supplement, the population densities in the YRD region are larger in  
309 Shanghai, southern Jiangsu and northern Zhejiang.

310 Finally, the year of life lost (YLL) due to  $PM_{2.5}$  exposure was calculated following  
311 eq. (4), where  $N$  represent the number of deaths in each age-gender-specific group,  
312 and  $L$  reflects the remaining life expectancy of the group:

$$313 \quad YLL = \sum_{i,j} N_{i,j} \times L_{i,j} \quad (4)$$

314 The remaining life expectancies by age were obtained from the life tables from  
315 the World Health Organization (WHO, <https://www.who.int>), as summarized in Table  
316 S5 in the Supplement. The life expectancies at birth of Chinese males and females in  
317 2015 were 74.8 and 77.7 years, respectively.



### 318 **3. Results and discussion**

#### 319 **3.1 Evaluation of emission estimates with air quality simulation**

##### 320 **3.1.1 Model performances without/with CEMS data**

321 Air quality simulations based on emission inventories without/with incorporation  
322 of CEMS data for the coal-fired power sector (Cases 1 and 2, respectively) were  
323 conducted to test the improvement of emission estimates. Because of the combined  
324 influences of regional transport and chemical reactions of air pollutants in the  
325 atmosphere, nonlinear relationships were found between the changes of primary  
326 emissions and ambient concentrations of air pollutants. Compared to Case 1, the  
327 simulated annual average concentrations of SO<sub>2</sub>, NO<sub>2</sub> and PM<sub>2.5</sub> in the YRD region  
328 were 10%, 7% and 6% lower respectively in Case 2, while that of O<sub>3</sub> was 7% higher,  
329 due to combined effects of emissions of volatile organic compounds (VOCs) and NO<sub>x</sub>  
330 precursors (Gao et al., 2005; Yang et al., 2012). Previous studies have shown that O<sub>3</sub>  
331 formation in most of the YRD region is under the “VOCs-limited” regime, i.e., the  
332 generation and removal of O<sub>3</sub> is more sensitive to VOCs and would be inhibited with  
333 high NO<sub>x</sub> concentrations in the atmosphere (Zhang et al., 2008; Liu et al., 2010;  
334 Wang et al., 2010; Xing et al., 2011). Therefore, the simulated reduced NO<sub>2</sub>  
335 concentrations from greater NO<sub>x</sub> emission control could elevate the O<sub>3</sub> concentration.

336 The simulated concentrations of SO<sub>2</sub>, NO<sub>2</sub>, O<sub>3</sub> and PM<sub>2.5</sub> based on the two  
337 emission inventories without/with CEMS data were compared with ground  
338 observations and are summarized in Table 2. Similar model performances were found  
339 for the two emission cases, with overestimation of SO<sub>2</sub>, NO<sub>2</sub> and PM<sub>2.5</sub> and  
340 underestimation of O<sub>3</sub>. The NMEs between the simulated and observed SO<sub>2</sub>, O<sub>3</sub> and  
341 PM<sub>2.5</sub> concentrations were all smaller than 50% for both cases, and slightly worse  
342 simulation performances were found in July compared to the other three months. In  
343 particular, the correlation coefficients (R) between the simulated and observed SO<sub>2</sub> in  
344 July were only 0.17 and 0.14 for Cases 1 and 2, respectively, and the NMEs between  
345 the simulated and observed NO<sub>2</sub> were larger than 100%. In addition, greater  
346 overestimation of SO<sub>2</sub> and PM<sub>2.5</sub> by the model was found in July than other months,  
347 likely attributable to bias of WRF modeling. On one hand, the simulated WS10 in the  
348 YRD region in July (2.67 m/s) was slightly lower than the observation (2.75 m/s). The



349 underestimation in wind speed could weaken the horizontal diffusion and lead to  
350 overestimation in air pollutant concentrations. Compared with the results from the  
351 European Centre for Medium-range Weather Forecasts (ECMWF,  
352 <https://apps.ecmwf.int/datasets>), on the other hand, the simulated boundary layer  
353 height (BLH) was lower in WRF for all months. The NMBs of the WRF and ECMWF  
354 BLH in January, April and October were around -15%, while that in July reached  
355 -24%. The lower BLH would limit the vertical convection and diffusion of pollutants,  
356 and thereby increase the surface concentrations of air pollutants. Similar to previous  
357 studies (An et al., 2013; Liao et al., 2015; Tang et al., 2015; Gao et al., 2016; Wang et  
358 al., 2016; Zhou et al., 2017), underestimation of O<sub>3</sub> was commonly found, and the  
359 NMBs and NMEs between the simulation and observation for the two cases ranged  
360 from -34.5% to 1.6% and from 27.5% to 37.1%, respectively. The underestimation in  
361 O<sub>3</sub> likely resulted from bias in the estimation of precursor emissions. Suggested by the  
362 positive NMBs of NO<sub>2</sub> modeling in Table 2, the NO<sub>x</sub> emissions were expected to be  
363 overestimated in the two cases, even for Case 2 with the CEMS data incorporated  
364 (which reflect the emission control benefits in recent years, as discussed in Y. Zhang  
365 et al., 2019). In addition, underestimation of VOC emissions is likely due to  
366 incomplete accounting of emission sources, particularly for uncontrolled or fugitive  
367 leakage (Zhao et al, 2017). In a VOC-limited regime, therefore, the overestimation of  
368 NO<sub>x</sub> and underestimation of VOCs would contribute to lower simulated O<sub>3</sub>  
369 concentrations than observations. In general, the simulations of both cases captured  
370 well the temporal variations of PM<sub>2.5</sub> concentrations, with the R between the observed  
371 and simulated concentrations around 0.9.

372 In general, better modeling performance in the YRD region was found in Case 2  
373 than Case 1. The monthly average NMBs between the simulated and observed  
374 concentrations of SO<sub>2</sub>, NO<sub>2</sub>, O<sub>3</sub> and PM<sub>2.5</sub> were -3.1%, 56.3%, -19.5% and -1.4% for  
375 Case 2, smaller in absolute value than those for Case 1 at 8.2%, 68.9%, -24.6% and  
376 7.6%, respectively. The bootstrap sampling (Gleser et al., 1996; He et al., 2017) was  
377 further applied to test the significance of the improvements of Case 2 over Case 1. (A  
378 significant difference is demonstrated if the confidence intervals of given statistical  
379 indices sampled from the two cases do not overlap.) As can be seen in Table 2, the  
380 modeling performances of the concerned species in Case 2 were improved  
381 significantly in most instances compared to Case 1. For example, the improvement of



382 NMB for the  $\text{SO}_2$  simulation was significant at the 99% confidence level for July and  
383 October, and 95% for January. The improvement of NMB and NME for  $\text{NO}_2$  was  
384 significant at confidence levels of 99% and 95% respectively for April. The  
385 improvement of NMB for  $\text{O}_3$  was significant at the 95% confidence level for January,  
386 and that of  $\text{PM}_{2.5}$  at 95% for April and 99% for July. The statistical test confirms that  
387 incorporation of online monitoring data in the emission inventory can improve the  
388 regional air quality modeling for the YRD region

389 Figure 2 illustrates the spatial patterns of the simulated monthly  $\text{SO}_2$ ,  $\text{NO}_2$ ,  $\text{O}_3$   
390 and  $\text{PM}_{2.5}$  concentrations for Case 2. For a given species, similar patterns were found  
391 for different months. In general, the simulated concentrations of  $\text{SO}_2$ ,  $\text{NO}_2$  and  $\text{PM}_{2.5}$   
392 were larger in central and northern Anhui, southern Jiangsu, Shanghai and coastal  
393 areas in Zhejiang, where large power and industrial plants are concentrated, as shown  
394 in Figure S2 in the Supplement. In the highly populated cities (Shanghai, Nanjing,  
395 Hangzhou, and Hefei; see their locations in Figure 1), the simulated concentrations of  
396 pollutants were significantly larger than their surrounding areas. For example, the  
397 simulated  $\text{SO}_2$ ,  $\text{NO}_2$  and  $\text{PM}_{2.5}$  concentrations in Nanjing were 1.4, 1.3 and 1.2 times  
398 of those in its nearby cities. The analogous numbers for Hangzhou were 2.5, 1.5 and  
399 1.3. In contrast, the simulated  $\text{O}_3$  concentrations were smaller in urban areas and  
400 larger in suburban ones. For instance, the simulated  $\text{O}_3$  in Nanjing, Shanghai, Hefei  
401 and Hangzhou were 0.7, 0.4, 0.6 and 0.6 times of those in their surrounding areas,  
402 respectively. The spatial distributions of the simulated  $\text{NO}_2$  and  $\text{O}_3$  concentrations in  
403 Figure 2 also indicated that  $\text{O}_3$  concentrations were less in the regions with higher  
404  $\text{NO}_2$  concentrations, such as the megacity of Shanghai. The simulated high  
405 concentrations of  $\text{NO}_2$  in urban areas promotes titration of  $\text{O}_3$ , reducing its  
406 concentrations. In addition,  $\text{O}_3$  concentrations could remain relatively high after  
407 transport from urban to the suburban areas due to relatively small emissions of  $\text{NO}_x$   
408 in the latter.

### 409 3.1.2 Benefits of the “ultra-low” emission controls on air quality

410 Table 3 summarizes the absolute and relative changes of the simulated monthly  
411 concentrations of the concerned air pollutants in Cases 3-5 compared to the base case  
412 (Case 2). The average contributions of the power sector to the total ambient  
413 concentrations of  $\text{SO}_2$ ,  $\text{NO}_2$  and  $\text{PM}_{2.5}$  for the four simulated months are estimated at



414 10.0%, 4.7%, and 2.3%, respectively, based on comparison of Cases 2 and 5. The  
415 contributions to the concentrations were close to those of emissions at 10.7%, 6.6%,  
416 and 1.6% for the three species (as indicated in Table S2), respectively. The larger  
417 power sector contribution to the ambient  $PM_{2.5}$  concentrations than to primary PM  
418 emissions reflects high emissions of precursors of secondary sulfate and nitrate  
419 aerosols. In general, limited contributions from the power sector were found for all  
420 concerned species except  $SO_2$ , attributed to the gradually improved controls in the  
421 sector. The further implementation of the ultra-low emission policy in the sector,  
422 therefore, is expected to result in limited additional benefits for air quality. As shown  
423 in Table 3, the absolute changes of the simulated  $SO_2$ ,  $NO_2$ ,  $O_3$  and  $PM_{2.5}$   
424 concentrations in Case 3 compared to Case 2 were all smaller than  $1 \mu\text{g}/\text{m}^3$  for the  
425 four months. Larger changes were found for primary pollutants ( $SO_2$  and  $NO_2$ ) than  
426 those of secondary ones ( $O_3$  and  $PM_{2.5}$ ): the simulated monthly concentrations of  $SO_2$   
427 and  $NO_2$  were 2.7%-6.1% and 2.0%-2.9% lower, while  $PM_{2.5}$  was only 0.1%-1.3%  
428 lower and  $O_3$  0.8%-2.2% higher, respectively. Much larger benefits were found when  
429 the ultra-low emission policy was broadened from the power sector to the industrial  
430 sector (Case 4), attributed to the dominant role of industry in air pollutant emissions in  
431 the YRD region (Table S2). The simulated monthly concentrations of  $SO_2$ ,  $NO_2$  and  
432  $PM_{2.5}$  were 1.5-2.0, 2.5-3.7, and 4.6-6.5  $\mu\text{g}/\text{m}^3$  lower compared to the base case,  
433 respectively, or reduction rates of 32.9%-64.1%, 16.4%-22.8%, and 6.2%-21.6%. In  
434 contrast, the simulated  $O_3$  concentration was 0.8-4.8  $\mu\text{g}/\text{m}^3$  higher, with growth rates  
435 ranging 2.6%-14.0%. As mentioned earlier, the YRD was identified as a VOC-limited  
436 region, and reducing  $NO_x$  emissions without any VOC controls would enhance  $O_3$   
437 concentrations. In order to alleviate regional air pollution including  $O_3$ , therefore,  
438 coordinated controls of  $NO_x$  and VOC emissions are urgently required. These would  
439 include measures to reduce large sources of VOCs, notably in non-power industries  
440 such as chemicals and refining and in solvent use (Zhao et al., 2017).

441 The relative changes in the simulated pollutant concentrations varied by month,  
442 due to the combined influences of meteorology and secondary chemistry, and larger  
443 changes were found for  $SO_2$  and  $PM_{2.5}$  in summer. As shown in Table 3, for example,  
444 the average simulated  $PM_{2.5}$  concentrations in July were 0.4 and 6.5  $\mu\text{g}/\text{m}^3$  lower  
445 respectively under Cases 3 and 4 compared to Case 2, with the larger reduction than  
446 other three months. This could result partly from the faster response of ambient



447 concentrations to the changed emissions of air pollutants with shorter lifetimes in  
448 summer. Moreover, the formation of secondary pollutants like PM<sub>2.5</sub> would be  
449 enhanced in summer, with more oxidative atmospheric conditions under high  
450 temperature and strong sunlight.

451 Figures 3 and 4 illustrate the spatial distributions of the relative changes of  
452 simulated pollutant concentrations in Cases 3 and 4 compared to Case 2, respectively.  
453 As shown in Figure 3, the overall changes across the region due to ultra-low emission  
454 controls in the power sector only were less than 10% for primary pollutants SO<sub>2</sub> and  
455 NO<sub>2</sub>, and 5% for secondary pollutants PM<sub>2.5</sub> and O<sub>3</sub>. Larger changes in simulated SO<sub>2</sub>  
456 concentrations were found in central and northern Anhui as well as central and  
457 southern Jiangsu, with relatively concentrated distribution of coal-fired power plants.  
458 The changes of simulated SO<sub>2</sub> and NO<sub>2</sub> in Shanghai were tiny, due to few remaining  
459 power plants subject to the ultra-low emission policy and thus few emission  
460 reductions. Compared to Case 2, the SO<sub>2</sub> and NO<sub>x</sub> emissions in Case 3 were  
461 estimated to be 2.2% and 0.8% lower respectively for Shanghai, much smaller than  
462 for other provinces (6.1% and 2.5% for Anhui, 9.5% and 4.4% for Jiangsu, 5.5% and  
463 2.7% for Zhejiang). The results suggest that the potential of emission reduction and  
464 air quality improvement is limited from implementation of more stringent control  
465 measures in the power sector alone, particularly in highly developed cities where air  
466 pollution controls have already reached a relatively high level.

467 In Case 4, where both power plant and industrial boilers meet the ultra-low  
468 emission requirement, the average reduction rates of simulated SO<sub>2</sub> and NO<sub>2</sub>  
469 concentrations compared to Case 2 were above 40% and 25% respectively for the  
470 whole region, and the changes of secondary pollutants O<sub>3</sub> and PM<sub>2.5</sub> were also  
471 significantly larger than those of Case 3 in most of the region. The relative changes of  
472 SO<sub>2</sub> were found to be more significant than other species, as the SO<sub>2</sub> concentrations  
473 are greatly affected by primary emissions. Due to the large number and wide  
474 distribution of industrial plants throughout the YRD, moreover, there was little  
475 regional disparity in the changed ambient SO<sub>2</sub> levels. In the central YRD, including  
476 Shanghai, northern Zhejiang and southern Jiangsu, the changes in simulated NO<sub>2</sub> were  
477 modest, resulting in clear enhancement of O<sub>3</sub> concentrations. The result suggests the  
478 great challenges of O<sub>3</sub> pollution abatement in those developed areas, even with  
479 aggressive measures on NO<sub>x</sub> control at power and industrial plants.



## 480 **3.2 Evaluation of health benefits**

### 481 **3.2.1 PM<sub>2.5</sub> exposures in the YRD region**

482 Figure 5 illustrates the spatial distributions of PM<sub>2.5</sub> concentrations for the base  
483 case (Case 2) and the differences of Cases 3 and 4 compared to the base case. The  
484 reduction of PM<sub>2.5</sub> concentrations from the implementation of the ultra-low emission  
485 policy in the power sector was less than 1 µg/m<sup>3</sup> over the YRD region (Figure 5b).  
486 Larger reductions (above 0.4 µg/m<sup>3</sup>) were found in northern Anhui and northern and  
487 southern Jiangsu provinces, as those regions are the energy base of eastern China,  
488 with abundant coal mines and power plants with large installed capacities. With the  
489 policy expanded to industrial boilers, the simulated average PM<sub>2.5</sub> concentrations were  
490 5.8 µg/m<sup>3</sup> lower for the whole region (Figure 5c). In particular, the difference was  
491 greater than 10 µg/m<sup>3</sup> along the Yangtze River, as there are many industrial parks  
492 located along the river containing a large number of big cement, iron & steel, and  
493 chemical industry plants. Stringent emission controls at those plants would result in  
494 significant benefits in air quality for local residents.

495 We further calculated the fractions of the population with different annual  
496 average PM<sub>2.5</sub> exposure levels in Cases 2-4, as shown in Figure 6. Compared to Case  
497 2, slight differences in the population distribution by exposure level were found in  
498 Case 3, while the differences were much more significant in Case 4. The population  
499 fractions exposed to the average annual concentrations of PM<sub>2.5</sub> smaller than 35 µg/m<sup>3</sup>,  
500 35-45 µg/m<sup>3</sup> and 45-55 µg/m<sup>3</sup> were estimated to grow from 14% in Case 2 to 21% in  
501 Case 4, from 11% to 16%, and from 16% to 30%, respectively. Accordingly, the  
502 fraction exposed to PM<sub>2.5</sub> concentrations larger than 55 µg/m<sup>3</sup> declined from 59% to  
503 33%. The implementation of ultra-low emission policy on both power plants and  
504 industry sectors thus proved an effective way in limiting the population exposed to  
505 high PM<sub>2.5</sub> levels.

### 506 **3.2.2 Human health risk with base case emissions**

507 The mortality and YLL caused by atmospheric PM<sub>2.5</sub> exposure with the base case  
508 emissions (Case 2) in the YRD region are shown in Table 4. The values in brackets  
509 represent the 95% confidence interval (CI) attributed to the uncertainty of IER curves



510 (i.e., uncertainties from other sources were excluded in the 95% CI estimation such as  
511 air quality model mechanisms, emission inventories, and population data). With the  
512 base case emissions, the NMB of the simulated and observed annual  $PM_{2.5}$   
513 concentrations (based on the four representative months) was calculated at -1.4% for  
514 the YRD region. Therefore, the influence of the biases between the simulations and  
515 observations on the estimated health risks was negligible and thus not considered in  
516 this study. The total attributable deaths due to all diseases caused by  $PM_{2.5}$  exposure in  
517 the YRD region were estimated at 194,000 (114,000-282,000), with STK, IHD and  
518 COPD causing the most deaths, accounting for 29%, 32% and 22% of the total  
519 respectively. With larger populations in Anhui and Jiangsu (32% and 37% of the  
520 regional total respectively), more deaths caused by  $PM_{2.5}$  exposure were found in  
521 these two provinces, at 34% and 41% of the total deaths respectively. Among all the  
522 diseases, STK was found to cause the largest number of mortalities (19,600) in Anhui  
523 with  $PM_{2.5}$  exposure, IHD in Jiangsu (31,300), and COPD in Shanghai (4,400) and  
524 Zhejiang (10,800). The total YLL caused by  $PM_{2.5}$  exposure in the YRD region was  
525 5.11 million years (3.16 - 7.18 million years). More YLL caused by  $PM_{2.5}$  exposure  
526 was found in Anhui and Jiangsu, accounting for 34% and 37% of the total in the YRD  
527 region respectively. YLL caused by COPD were the largest in all the provinces, with  
528 0.66, 0.19, 0.56 and 0.47 million years estimated for Anhui, Shanghai, Jiangsu and  
529 Zhejiang, respectively. The spatial distribution of attributable deaths and YLL caused  
530 by  $PM_{2.5}$  exposure was basically consistent with that of population in the YRD region,  
531 with correlation coefficients of 0.94 and 0.96 respectively. As shown in Figure 7,  
532 higher health risks attributed to  $PM_{2.5}$  pollution under the base case (Case 2) were  
533 found in the areas along the Yangtze River, central Shanghai and some urban areas in  
534 Anhui, all with higher population densities. We further compared the population  
535 deaths attributable to  $PM_{2.5}$  exposure calculated in this study with the reported total  
536 deaths in provincial statistical yearbooks (AHBS, 2016; JSBS, 2016; SHBS, 2016;  
537 ZJBS, 2016), and found that the deaths caused by  $PM_{2.5}$  exposure accounted for 18%,  
538 14%, 15% and 11% of the total deaths in Anhui, Jiangsu, Shanghai and Zhejiang  
539 respectively for 2015. The numbers were larger than the estimate (6.9%) by Maji et al.  
540 (2018), which focused on 161 cities in China.

541 Many studies have focused on the human health risks attributable to air pollution  
542 in China, with considerable disparities between them due to different estimation



543 methods and health endpoints selected. Figure 8 compares the estimates of premature  
544 deaths caused by  $PM_{2.5}$  exposure in the YRD region in this and previous studies.  
545 Relatively close results are found between studies for the same regions and periods.  
546 For example, Hu et al. (2017) and Liu et al. (2016) estimated that the premature  
547 deaths of adults (>30 years old) due to  $PM_{2.5}$  exposure were 223,000 and 245,000  
548 respectively in 2013 in the YRD region. However, the health endpoints in these two  
549 studies were not completely consistent. COPD, LC, IHD and CEV (cerebrovascular  
550 disease) were selected in Hu et al. (2017), while COPD, LC, IHD and STK were  
551 chosen by Liu et al. (2016). The deaths caused by  $PM_{2.5}$  exposure in Shanghai were  
552 estimated at 19,000, 15,000, and 16,000 respectively in Maji et al. (2018), Song et al.  
553 (2017) and this study, respectively. The IER model and the same health endpoints  
554 were adopted in all three studies, while the  $PM_{2.5}$  concentrations were derived from  
555 ground observations in the former two studies instead of air quality simulation in this  
556 study. The premature deaths attributable to  $PM_{2.5}$  exposure in the YRD region in 2015  
557 were estimated at 122,000 in Maji et al. (2018) and 194,000 in this study respectively,  
558 with the discrepancy resulting in part from inclusion of only typical cities instead of  
559 all cities of the YRD region in the estimation of the former. There are clear disparities  
560 in estimates of premature deaths for different years. For example, the death estimates  
561 caused by  $PM_{2.5}$  exposure in 2015 were generally smaller than those in 2013. As the  
562 population and age distributions remained relatively stable over the two years (AHBS,  
563 2016; JSBS, 2016; SHBS, 2016; ZJBS, 2016), the reduced estimated premature  
564 deaths result to some extent from emission abatement and air quality improvement.  
565 According to relevant studies of Shanghai in particular (Lelieveld et al., 2013; 2015;  
566 Liu et al., 2016; Xie et al., 2016; Hu et al., 2017; Song et al., 2017; Maji et al., 2018),  
567 the premature deaths attributable to  $PM_{2.5}$  exposure increased from 2005 to 2013 and  
568 then declined afterwards, reflecting the health benefit of air pollution control  
569 measures in Shanghai in recent years.

### 570 **3.2.3 Benefits of emission controls on human health**

571 Tables 5 and 6 respectively summarize the avoided premature deaths and YLL by  
572 disease and region that would result from implementation of the ultra-low emission  
573 control policy and thereby reduced  $PM_{2.5}$  pollution in the YRD region. If only the  
574 coal-fired power sector meet the ultra-low emission limits (Case 3), nearly 305



575 premature deaths would be avoided compared to the base case emissions in 2015,  
576 with a tiny reduction rate of only 0.16%. If the policy is strictly implemented for the  
577 industrial sector as well (Case 4), 10,651 premature deaths could be avoided with a  
578 reduction rate at 5.50%. The largest numbers of avoided premature deaths were found  
579 in Anhui and Jiangsu, accounting collectively for 88.2% and 68.7% of the total  
580 avoided deaths in Cases 3 and 4 respectively. The greatest impacts from reduced  
581  $PM_{2.5}$  concentrations were found for STK, of which the avoided deaths were  
582 calculated at 85 and 2848 in Cases 3 and 4, respectively. The health effects of  
583 emission control policies in the YRD region have been investigated in previous  
584 studies. Using the IER model, Dai et al. (2019) chose the premature deaths from IHD,  
585 CEV, COPD and LC as health endpoints, and found that the Clean Air Action Plan  
586 would avoid 3,439 deaths caused by  $PM_{2.5}$  exposure in Shanghai, more than those in  
587 both Case 3 and Case 4 in this study (5 and 1,185 respectively). Applying  
588 environmental health risk and valuation methods, Li and Li (2018) found that 15,709  
589 premature deaths attributable to air pollution could be avoided in 2015 if the  $PM_{2.5}$   
590 concentrations in Jiangsu province were assumed to meet the National Ambient Air  
591 Quality Standard (GB3095-2012,  $35 \mu\text{g}/\text{m}^3$  as the annual average). The estimate is  
592 much more than those calculated in Case 3 and Case 4 (177 and 4,114 deaths  
593 respectively). The larger health benefits estimated in those two studies result from  
594 their assumption of emission control measures covering a much wider range of sectors  
595 including energy, industry, transportation, construction, and agriculture, while only the  
596 ultra-low emission policy was assumed for the power and industry sectors in this  
597 study. The comparisons illustrate that the health benefits from emission control in the  
598 power sector alone is limited, and that controls in other sectors are essential. In  
599 addition, the different methods and inconsistent data sources partly led to the  
600 discrepancies. For the particle exposure estimation, as an example, Dai et al. (2019)  
601 adopted the BENMAP-CE model (Environmental Benefits Mapping and Analysis  
602 Program-Community Edition, Yang et al. (2013)) to simulate the ambient  $PM_{2.5}$   
603 concentrations, while Li and Li (2018) used the average of monitored  $PM_{2.5}$   
604 concentrations. As shown in Table 6, the avoided YLL for Case 3 and Case 4 were  
605 estimated at 8744 and 316,562 years respectively compared to the base case,  
606 confirming again the greatly improved health benefits from implementation of  
607 ultra-low emission policy for the industry sector in addition to the power sector. The



608 largest avoided YLL were found in Anhui and Jiangsu in the YRD region, accounting  
609 collectively for 86% and 65% of the total avoided YLL in Cases 3 and 4 respectively.  
610 Comparing Case 3 to Case 4, the fractions of both avoided deaths and YLL were  
611 clearly higher for Shanghai and part of Zhejiang, implying a greater health benefit of  
612 emission controls at industry sources in these relatively industrialized urban regions.  
613 The reduced  $PM_{2.5}$  concentrations led to the largest avoided YLL of COPD in both  
614 cases (3,118 and 119,300 years in Cases 3 and 4, respectively).

615 Figure 9 illustrates the spatial distributions of the avoided deaths and YLL from  
616 the ultra-low emission policy in the YRD region. When the policy was implemented  
617 only for coal-fired power plants, the health benefits were small and the regional  
618 differences relatively insignificant, with the avoided deaths and YLL smaller than 10  
619 persons and 100 years respectively for all of the grid cells (Figure 9a and 9b). When  
620 the policy was implemented both in power and industry sectors, more avoided deaths  
621 ( $>40$  person/grid cell) and YLL ( $>400$  years/grid cell) were found in northern Anhui,  
622 southern Jiangsu, central Shanghai and northern Zhejiang (Figure 9c and 9d). The  
623 spatial correlation coefficient between the avoided YLL in Case 4 and population was  
624 0.93, indicating that the implementation of the emission control policy would lead to  
625 greater health benefits for areas with intensive economic activity and dense  
626 populations.

627

#### 628 4. Conclusions

629 We evaluated the improvement of emission estimation by incorporating CEMS  
630 data for the power sector, and explored the air quality and health benefits from the  
631 ultra-low emission control policy for the YRD region through air quality modeling. In  
632 general, the bias between ground observations and simulations based on the emission  
633 inventory with CEMS data incorporated was smaller than that without, suggesting that  
634 appropriate use of online monitoring information helped improve the emission  
635 estimation and model performance. Compared to the base case in which CEMS data  
636 were incorporated in emission estimation, the simulated monthly concentrations of all  
637 the concerned species ( $SO_2$ ,  $NO_2$ ,  $O_3$ , and  $PM_{2.5}$ ) differed less than 7% when the  
638 ultra-low emission policy was enacted only in the coal-fired power sector, given its  
639 small fraction of total emissions. When the policy was implemented for the industrial



640 sector as well, larger differences in air quality from the base case were found, with the  
641 simulated concentrations of SO<sub>2</sub>, NO<sub>2</sub> and PM<sub>2.5</sub> respectively 33%-64%, 16%-23%  
642 and 6%-22% lower and O<sub>3</sub> 3%-14% higher, depending on the month.

643 Nearly 305 premature deaths and 8,744 years of YLL would be avoided if the  
644 policy was implemented for the power sector alone, and benefits would reach 10,651  
645 premature deaths and 316,562 YLL avoided with the policy enacted for both power  
646 and industry sectors. The study revealed the limited potential for further emission  
647 reduction and air quality improvement via controls in the power sector alone. Along  
648 with stringent emission control in that sector, the coordinated control of emissions  
649 from non-power industrial sources would be essential to effectively improve air  
650 quality and reduce associated human health risks. Moreover, more attention needs to  
651 be paid to control of VOC to limit O<sub>3</sub> formation resulting from reduction of NO<sub>x</sub> in  
652 the region.

653

## 654 **Data availability**

655 All data in this study are available from the authors upon request.

## 656 **Author contributions**

657 YZhang developed the strategy and methodology of the work and wrote the draft.  
658 YZhao improved the methodology and revised the manuscript. MG provided useful  
659 comments on the health risk analysis. XB provided emission monitoring data. CPN  
660 revised the manuscript.

## 661 **Competing interests**

662 The authors declare that they have no conflict of interest.

## 663 **Acknowledgments**

664 This work was sponsored by the Natural Science Foundation of China (41922052 and  
665 91644220), National Key Research and Development Program of China  
666 (2017YFC0210106), and a Harvard Global Institute award to the Harvard-China



667 Project on Energy, Economy and Environment. We would also like to thank Tsinghua  
668 University for the free use of national emissions data (MEIC).

## 669 **References**

- 670 An, X., Sun, Z., Lin, W., Jin, M., and Li, N.: Emission inventory evaluation using  
671 observations of regional atmospheric background stations of China, *J. Environ.*  
672 *Sci.*, 25, 537-536, 2013.
- 673 AHBS (Anhui Bureau of Statistics): Statistical Yearbook of Anhui, China Statistics  
674 Press, Beijing, 2016 (in Chinese).
- 675 Baker, K., Johnson, M., and King, S.: Meteorological modeling performance  
676 summary for application to PM<sub>2.5</sub>/haze/ozone modeling projects, Lake Michigan  
677 Air Directors Consortium, Midwest Regional Planning Organization, Des Plaines,  
678 Illinois, USA, 57 pp, 2004.
- 679 Butt, E. W., Turnock, S. T., Rigby, R., Reddington, C. L., Yoshioka, M., Johnson, J. S.,  
680 Regayre, L. A., Pringle, K. J., Mann, G. W., and Spracklen, D. V.: Global and  
681 regional trends in particulate air pollution and attributable health burden over the  
682 past 50 years, *Environ. Res. Lett.*, 12, 10.1088/1748-9326/aa87be, 2017.
- 683 Chang, X., Wang, S., Zhao, B., Xing, J., Liu, X., Wei, L., Song, Y., Wu, W., Cai, S.,  
684 Zheng, H., Ding, D., and Zheng, M.: Contributions of inter-city and regional  
685 transport to PM<sub>2.5</sub> concentrations in the Beijing-Tianjin-Hebei region and its  
686 implications on regional joint air pollution control, *Sci. Total. Environ.*, 660,  
687 1191-1200, 10.1016/j.scitotenv.2018.12.474, 2019.
- 688 Cohen, A. J., Brauer, M., Burnett, R., Anderson, H. R., Frostad, J., Estep, K., et al.:  
689 Estimates and 25-year trends of the global burden of disease attributable to  
690 ambient air pollution: an analysis of data from the Global Burden of Diseases  
691 Study 2015, *Lancet*, 389, 1907-1918, 2017.
- 692 Dai, H. X., An, J. Y., Li, L., Huang, C., Yan, R. S., Zhu, S. H., Ma, Y. G., Song, W. M.,  
693 and Kan, H. D.: Health Benefit Analyses of the Clean Air Action Plan  
694 Implementation in Shanghai, *Environmental Science*, 40, 1, 10.13227  
695 /j.hjlx.201804201, 2019 (in Chinese).
- 696 Dockery, D. W., Pope, C. A., Xu, X. P., Spengler, J. D., Ware, J. H., Fay, M. E., Ferris,  
697 B. G., and Speizer, F. E.: An Association between air-pollution and mortality in 6  
698 United-States cities, *N. Engl. J. Med.*, 329, 1753-1759,



- 699 10.1056/nejm199312093292401, 1993.
- 700 Emery, C., Tai, E., and Yarwood, G.: Enhanced meteorological modeling and  
701 performance evaluation for two Texas episodes, Report to the Texas Natural  
702 Resources Conservation Commission, prepared by ENVIRON, International  
703 Corp, Novato, CA, 2001.
- 704 Fu, J. S., Jang, C. J., Streets, D. G., Li, Z., Kwok, R., Park, R., and Han, Z.:  
705 MICS-Asia II: Modeling gaseous pollutants and evaluating an advanced  
706 modeling system over East Asia, *Atmos. Environ.*, 42, 3571-3583,  
707 10.1016/j.atmosenv.2007.07.058, 2008.
- 708 Gao, J., Wang, T., Ding, A. J., and Liu, C. B.: Observational study of ozone and  
709 carbon monoxide at the summit of mount Tai (1534 m a.s.l.) in central-eastern  
710 China, *Atmos. Environ.*, 39, 4779-4791, 10.1016/j.atmosenv.2005.04.030, 2005.
- 711 Gao, J. H., Zhu, B., Xiao, H., Kang, H. Q., Hou, X. W., and Shao, P.: A case study of  
712 surface ozone source apportionment during a high concentration episode, under  
713 frequent shifting wind conditions over the Yangtze River Delta, China, *Sci. Total  
714 Environ.*, 544, 853-863, 2016.
- 715 Gao, M., Beig, G., Song, S., Zhang, H., Hu, J., Ying, Q., Liang, F., Liu, Y., Wang, H.,  
716 Lu, X., Zhu, T., Carmichael, G. R., Nielsen, C. P., and McElroy, M. B.: The  
717 impact of power generation emissions on ambient PM<sub>2.5</sub> pollution and human  
718 health in China and India, *Environ. Int.*, 121, 250-259,  
719 10.1016/j.envint.2018.09.015, 2018.
- 720 Gleser, L. J.: Bootstrap confidence intervals, *Statistical Science*, 11, 219-221, 1996.
- 721 Guenther, A. B., Jiang, X., Heald, C. L., Sakulyanontvittaya, T., Duhl, T., Emmons, L.  
722 K., and Wang, X.: The Model of Emissions of Gases and Aerosols from Nature  
723 version 2.1 (MEGAN2.1): an extended and updated framework for modeling  
724 biogenic emissions, *Geosci. Model Dev.*, 5, 1471-1492, 2012.
- 725 Han, K. M., Lee, S., Chang, L. S., and Song, C. H.: A comparison study between  
726 CMAQ-simulated and OMI-retrieved NO<sub>2</sub> columns over East Asia for evaluation  
727 of NO<sub>x</sub> emission fluxes of INTEX-B, CAPSS, and REAS inventories, *Atmos.  
728 Chem. Phys.*, 15, 1913-1938, 10.5194/acp-15-1913-2015, 2015.
- 729 He, J. J., Yu, Y., Yu, L. J., Liu, N., and Zhao, S. P.: Impacts of uncertainty in land  
730 surface information on simulated surface temperature and precipitation over  
731 China, *Int. J. Climatol.*, 10.1002/joc.5041, 2017.



- 732 Hoek, G., Krishnan, R. M., Beelen, R., Peters, A., Ostro, B., Brunekreef, B., and  
733 Kaufman, J. D.: Long-term air pollution exposure and cardio- respiratory  
734 mortality: a review, *Environmental Health*, 12, 10.1186/1476-069x-12-43, 2013.
- 735 Hu, J., Huang, L., Chen, M., Liao, H., and Ying, Q.: Premature mortality attributable  
736 to particulate matter in China: source contributions and responses to reductions,  
737 *Environ. Sci. Technol.*, 51, 9950-9959, 2017.
- 738 Huang, C., Chen, C. H., Li, L., Cheng, Z., Wang, H. L., Huang, H. Y., Streets, D. G.,  
739 Wang, Y. J., Zhang, G. F., and Chen, Y. R.: Emission inventory of anthropogenic  
740 air pollutants and VOC species in the Yangtze River Delta region, China, *Atmos.*  
741 *Chem. Phys.*, 11, 4105-4120, 10.5194/acp-11-4105-2011, 2011.
- 742 JSBS (Jiangsu Bureau of Statistics): *Statistical Yearbook of Jiangsu*, China Statistics  
743 Press, Beijing, 2016 (in Chinese).
- 744 Lei, Y., Xue, W. B., Zhang, Y. S., and Xu, Y. L.: Health benefit evaluation for air  
745 pollution prevention and control action plan in China, *Chinese Environmental*  
746 *Management*, 5, 10.16868/j.cnki.1674-6252.2015.05.009, 2015 (in Chinese).
- 747 Lelieveld, J., Barlas, C., Giannadaki, D., and Pozzer, A.: Model calculated global,  
748 regional and megacity premature mortality due to air pollution, *Atmos. Chem.*  
749 *Phys.*, 13, 7023-7037, 10.5194/acp-13-7023-2013, 2013.
- 750 Lelieveld, J., Evans, J. S., Fnais, M., Giannadaki, D., and Pozzer, A.: The contribution  
751 of outdoor air pollution sources to premature mortality on a global scale, *Nature*,  
752 525, 367-371, 10.1038/nature15371, 2015.
- 753 Li, H. J., and Li, M. Q.: Assessment on health benefit of air pollution control in  
754 Jiangsu province, *Chinese Public Health*, 34, 12, 10.11847/zgggws1117789,  
755 2018 (in Chinese).
- 756 Li, L., Chen, C. H., Fu, J. S., Huang, C., Streets, D. G., Huang, H. Y., Zhang, G. F.,  
757 Wang, Y. J., Jang, C. J., Wang, H. L., Chen, Y. R., and Fu, J. M.: Air quality and  
758 emissions in the Yangtze River Delta, China, *Atmos. Chem. Phys.*, 11,  
759 1621-1639, 10.5194/acp-11-1621-2011, 2011.
- 760 Li, L., Chen, C. H., Huang, C., Huang, H. Y., Zhang, G. F., Wang, Y. J., Wang, H. L.,  
761 Lou, S. R., Qiao, L. P., Zhou, M., Chen, M. H., Chen, Y. R., Streets, D. G., Fu, J.  
762 S., and Jang, C. J.: Process analysis of regional ozone formation over the Yangtze  
763 River Delta, China using the Community Multi-scale Air Quality modeling  
764 system, *Atmos. Chem. Phys.*, 12, 10971-10987, 10.5194/acp-12-10971-2012,



- 765 2012.
- 766 Li, L., An, J. Y., and Lu, Q.: Modeling Assessment of PM<sub>2.5</sub> Concentrations Under  
767 implementation of Clean Air Action Plan in the Yangtze River Delta Region,  
768 Research of Environmental Sciences, 28, 1653-1661,  
769 10.13198/j.issn.1001-6929.2015.11.01, 2015 (in Chinese).
- 770 Liao, J. B., Wang, T. J., Jiang, Z. Q., Zhuang, B. L., Xie, M., Yin, C. Q., Wang, X. M.,  
771 Zhu, J. L., Fu, Y., and Zhang, Y.: WRF/Chem modeling of the impacts of urban  
772 expansion on regional climate and air pollutants in Yangtze River Delta, China,  
773 Atmos. Environ., 106, 204-214, 10.1016/j.atmosenv.2015.01.059, 2015.
- 774 Lim, S. S., Vos, T., Flaxman, A. D., Danaei, G., Shibuya, K., Adair-Rohani, H., et al.:  
775 A comparative risk assessment of burden of disease and injury attributable to 67  
776 risk factors and risk factor clusters in 21 regions, 1990-2010: a systematic  
777 analysis for the Global Burden of Disease Study 2010, Lancet, 380, 2224-2260,  
778 2012.
- 779 Liu, J., Han, Y., Tang, X., Zhu, J., and Zhu, T.: Estimating adult mortality attributable  
780 to PM<sub>2.5</sub> exposure in China with assimilated PM<sub>2.5</sub> concentrations based on a  
781 ground monitoring network, Sci. Total Environ., 568, 1253-1262, 2016.
- 782 Liu, X., Gao, X., Wu, X., Yu, W., Chen, L., Ni, R., Zhao, Y., Duan, H., Zhao, F., Chen,  
783 L., Gao, S., Xu, K., Lin, J., and Ku, A. Y.: Updated Hourly Emissions Factors for  
784 Chinese Power Plants Showing the Impact of Widespread Ultralow Emissions  
785 Technology Deployment, Environ. Sci. Technol., 53, 2570-2578,  
786 10.1021/acs.est.8b07241, 2019.
- 787 Liu, X. H., Zhang, Y., Xing, J., Zhang, Q., Wang, K., Streets, D. G., Jiang, C., Wang,  
788 W. X., and Hao, J. M.: Understanding of regional air pollution over China using  
789 CMAQ, part II. Process analysis and sensitivity of ozone and particulate matter  
790 to precursor emissions, Atmos. Environ., 44, 3719-3727,  
791 10.1016/j.atmosenv.2010.03.036, 2010.
- 792 Maji, K. J., Dikshit, A. K., Arora, M., and Deshpande, A.: Estimating premature  
793 mortality attributable to PM<sub>2.5</sub> exposure and benefit of air pollution control  
794 policies in China for 2020, Sci. Total Environ., 612, 683-693,  
795 10.1016/j.scitotenv.2017.08.254, 2018.
- 796 Ohara, T., Akimoto, H., Kurokawa, J., Horii, N., Yamaji, K., Yan, X., and Hayasaka,  
797 T.: An Asian emission inventory of anthropogenic emission sources for the



- 798 period 1980-2020, *Atmos. Chem. Phys.*, 7, 4419-4444, 2007.
- 799 Price, C., Penner, J., and Prather, M.: NO<sub>x</sub> from lightning: 1. Global distribution  
800 based on lightning physics, *J. Geophys. Res.-Atmos.*, 102, 5929-5941,  
801 10.1029/96jd03504, 1997.
- 802 Shanghai Bureau of Statistics (SHBS): Statistical Yearbook of Shanghai, China  
803 Statistics Press, Beijing, 2016 (in Chinese).
- 804 Sindelarova, K., Granier, C., Bouarar, I., Guenther, A., Tilmes, S., Stavrou, T.,  
805 Muller, J. F., Kuhn, U., Stefani, P., and Knorr, W.: Global data set of biogenic  
806 VOC emissions calculated by the MEGAN model over the last 30 years, *Atmos.*  
807 *Chem. Phys.*, 14, 9317-9341, 10.5194/acp-14-9317-2014, 2014.
- 808 Skamarock, W. C., Klemp, J. B., Dudhia, J., Gill, D. O., Barker, D. M., Duda, M. G.,  
809 Huang, X.-Y., Wang, W., and Powers, J. G.: A Description of the Advanced  
810 Research WRF Version 3, NCAR Tech. Note NCAR/TN-475+STR, 113 pp.,  
811 10.5065/D68S4MVH, 2008.
- 812 Song, C., He, J., Wu, L., Jin, T., Chen, X., Li, R., Ren, P., Zhang, L., and Mao, H.:  
813 Health burden attributable to ambient PM<sub>2.5</sub> in China, *Environ. Pollut.*, 223,  
814 575-586, 2017.
- 815 Tan, J., Fu, J. S., Huang, K., Yang, C.-E., Zhuang, G., and Sun, J.: Effectiveness of  
816 SO<sub>2</sub> emission control policy on power plants in the Yangtze River Delta,  
817 China-post-assessment of the 11th Five-Year Plan, *Environ. Sci. Pollut. R.*, 24,  
818 8243-8255, 10.1007/s11356-017-8412-z, 2017.
- 819 Tang, L., Qu, J. B., Mi, Z. F., Bo, X., Chang, X. Y., Anadon, L. D., Wang, S. Y., Xue,  
820 X. D., Li, S. B., Wang, X., and Zhao, X. H.: Substantial emission reductions  
821 from Chinese power plants after the introduction of ultra-low emissions  
822 standards, *Nat. Energy*, 4, 929-938, 10.1038/s41560-019-0468-1, 2019.
- 823 Tang, Y., An, J., Wang, F., Li, Y., Qu, Y., Chen, Y., and Lin, J.: Impacts of an unknown  
824 daytime HONO source on the mixing ratio and budget of HONO, and hydroxyl,  
825 hydroperoxyl, and organic peroxy radicals, in the coastal regions of China,  
826 *Atmos. Chem. Phys.*, 15, 9381-9398, 10.5194/acp-15-9381-2015, 2015.
- 827 University of North Carolina at Chapel Hill (UNC): Operational Guidance for the  
828 Community Multiscale Air Quality (CMAQ) Modeling System Version 4.7.1  
829 (June 2010 Release), available at <http://www.cmaq-model.org> (last access: 10



- 830 Feb 2020), 2010.
- 831 Uno, I., He, Y., Ohara, T., Yamaji, K., Kurokawa, J. I., Katayama, M., Wang, Z.,  
832 Noguchi, K., Hayashida, S., Richter, A., and Burrows, J. P.: Systematic analysis  
833 of interannual and seasonal variations of model-simulated tropospheric NO<sub>2</sub> in  
834 Asia and comparison with GOME-satellite data, *Atmos. Chem. Phys.*, 7,  
835 1671-1681, 10.5194/acp-7-1671-2007, 2007.
- 836 Wang, G., Zhang, R., Gomez, M. E., Yang, L., Levy Zamora, M., Hu, M., et al.:  
837 Persistent sulfate formation from London Fog to Chinese haze. *P. Natl. Acad.*  
838 *Sci.*, 48, 13630-13635, 10.1073/pnas.1616540113, 2016.
- 839 Wang, K., Zhang, Y., Jang, C., Phillips, S., and Wang, B.: Modeling intercontinental  
840 air pollution transport over the trans-Pacific region in 2001 using the Community  
841 Multiscale Air Quality modeling system, *J. Geophys. Res.-Atmos.*, 114,  
842 10.1029/2008jd010807, 2009.
- 843 Wang, L. T., Jang, C., Zhang, Y., Wang, K., Zhang, Q., Streets, D. G., Fu, J., Lei, Y.,  
844 Schreifels, J., He, K. B., Hao, J. M., Lam, Y., Lin, J., Meskhidze, N., Voorhees, S.,  
845 Evarts, D., and Phillips, S.: Assessment of air quality benefits from national air  
846 pollution control policies in China. Part II: Evaluation of air quality predictions  
847 and air quality benefits assessment, *Atmos. Environ.*, 44, 3449-3457,  
848 10.1016/j.atmosenv.2010.05.051, 2010.
- 849 Wang, L. T., Wei, Z., Yang, J., Zhang, Y., Zhang, F. F., Su, J., Meng, C. C., and Zhang,  
850 Q.: The 2013 severe haze over southern Hebei, China: model evaluation, source  
851 apportionment, and policy implications, *Atmos. Chem. Phys.*, 14, 3151-3173,  
852 10.5194/acp-14-3151-2014, 2014.
- 853 Wang, Z., Pan, L., Li, Y., Zhang, D., Ma, J., Sun, F., Xu, W., and Wang, X.:  
854 Assessment of air quality benefits from the national pollution control policy of  
855 thermal power plants in China: A numerical simulation, *Atmos. Environ.*, 106,  
856 288-304, 10.1016/j.atmosenv.2015.01.022, 2015.
- 857 Xia, Y., Zhao, Y., and Nielsen, C. P.: Benefits of of China's efforts in gaseous pollutant  
858 control indicated by the bottom-up emissions and satellite observations  
859 2000-2014, *Atmos. Environ.*, 136, 43-53, 10.1016/j.atmosenv.2016.04.013, 2016.
- 860 Xie, R., Sabel, C. E., Lu, X., Zhu, W., Kan, H., Nielsen, C. P., and Wang, H.:  
861 Long-term trend and spatial pattern of PM<sub>2.5</sub> induced premature mortality in  
862 China, *Environ. Int.*, 97, 180-186, 10.1016/j.envint.2016.09.003, 2016.



- 863 Xing, J., Wang, S. X., Jang, C., Zhu, Y., and Hao, J. M.: Nonlinear response of ozone  
864 to precursor emission changes in China: a modeling study using response surface  
865 methodology, *Atmos. Chem. Phys.*, 11, 5027-5044, 10.5194/acp-11-5027-2011,  
866 2011.
- 867 Yang, C. F. O., Lin, N. H., Sheu, G. R., Lee, C. T., and Wang, J. L.: Seasonal and  
868 diurnal variations of ozone at a high-altitude mountain baseline station in East  
869 Asia, *Atmos. Environ.*, 46, 279-288, 10.1016/j.atmosenv.2011.09.060, 2012.
- 870 Yang, Y., Zhu, Y., Jang, C., Xie, J. P., Wang, S. X., Fu, J., Lin, C. J., Ma, J., Ding, D.,  
871 Qiu, X. Z., and Lao, Y. W.: Research and development of environmental benefits  
872 mapping and analysis program: Community edition, *Acta Scientiae*  
873 *Circumstantiae*, 33, 2395-2401, 10.13671/j.hjkxxb.2013.09.022, 2013 (in  
874 Chinese).
- 875 Yu, S., Mathur, R., Kang, D., Schere, K., Eder, B., and Pleirn, J.: Performance and  
876 diagnostic evaluation of ozone predictions by the eta-community multiscale air  
877 quality forecast system during the 2002 New England Air Quality Study, *J. Air*  
878 *Waste Manage.*, 56, 1459-1471, 10.1080/10473289.2006.10464554, 2006.
- 879 Zhang, L., Zhao, T., Gong, S., Kong, S., Tang, L., Liu, D., Wang, Y., Jin, L., Shan, Y.,  
880 Tan, C., Zhang, Y., and Guo, X.: Updated emission inventories of power plants in  
881 simulating air quality during haze periods over East China, *Atmos. Chem. Phys.*,  
882 18, 2065-2079, 10.5194/acp-18-2065-2018, 2018.
- 883 Zhang, M., Uno, I., Zhang, R., Han, Z., Wang, Z., and Pu, Y.: Evaluation of the  
884 Models-3 Community Multi-scale Air Quality (CMAQ) modeling system with  
885 observations obtained during the TRACE-P experiment: Comparison of ozone  
886 and its related species, *Atmos. Environ.*, 40, 4874-4882,  
887 10.1016/j.atmosenv.2005.06.063, 2006.
- 888 Zhang, Q., Streets, D. G., Carmichael, G. R., He, K. B., Huo, H., Kannari, A.,  
889 Klimont, Z., Park, I. S., Reddy, S., Fu, J. S., Chen, D., Duan, L., Lei, Y., Wang, L.  
890 T., and Yao, Z. L.: Asian emissions in 2006 for the NASA INTEX-B mission,  
891 *Atmos. Chem. Phys.*, 9, 5131-5153, 2009.
- 892 Zhang, Q., Zheng, Y., Tong, D., Shao, M., Wang, S., Zhang, Y., et al.: Drivers of  
893 improved PM<sub>2.5</sub> air quality in China from 2013 to 2017. *P. Natl. Acad. Sci.*, 116,  
894 24463-24469, 2019.
- 895 Zhang, X., Dai, H. C., Jin, Y. N., and Zhang, S. Q.: Evaluation of health and economic



- 896 benefits from “Coal to Electricity” Policy in the residential sector in the  
897 Jing-Jin-Ji Region, *Acta Scientiarum Naturalium Universitatis Pekinensis*, 55, 2,  
898 10.13209/j.0479-8023.2018.098, 2019 (in Chinese).
- 899 Zhang, Y., Bo, X., Zhao, Y., and Nielsen, C. P.: Benefits of current and future policies  
900 on emissions of China’s coal-fired power sector indicated by continuous emission  
901 monitoring, *Environ. Pollut.*, 251, 2019.
- 902 Zhang, Y. H., Su, H., Zhong, L. J., Cheng, Y. F., Zeng, L. M., and Wang, X. S.:  
903 Regional ozone pollution and observation-based approach for analyzing ozone–  
904 precursor relationship during the PRIDE-PRD2004 campaign, *Atmos. Environ.*,  
905 42, 6203-6218, 10.1016/j.atmosenv.2008.05.002, 2008.
- 906 Zhao, B., Wang, S. X., Dong, X. Y., Wang, J. D., Duan, L., Fu, X., Hao, J. M., and Fu,  
907 J.: Environmental effects of the recent emission changes in China: implications  
908 for particulate matter pollution and soil acidification, *Environ. Res. Lett.*, 8,  
909 10.1088/1748-9326/8/2/024031, 2013.
- 910 Zhao, Y., Zhang, J., and Nielsen, C. P.: The effects of recent control policies on trends  
911 in emissions of anthropogenic atmospheric pollutants and CO<sub>2</sub> in China, *Atmos.*  
912 *Chem. Phys.*, 13, 487-508, 10.5194/acp-13-487-2013, 2013.
- 913 Zhao, Y., Mao, P., Zhou, Y., Yang, Y., Zhang, J., Wang, S., Dong, Y., Xie, F., Yu, Y.,  
914 and Li W.: Improved provincial emission inventory and speciation profiles of  
915 anthropogenic non-methane volatile organic compounds: a case study for Jiangsu,  
916 China, *Atmos. Chem. Phys.*, 17, 7733-7756, 10.5194/acp-17-7733-2017, 2017.
- 917 Zheng, B., Zhang, Q., Tong, D., Chen, C., Hong, C., Li, M., Geng, G., Lei, Y., Huo,  
918 H., and He, K.: Resolution dependence of uncertainties in gridded emission  
919 inventories: a case study in Hebei, China, *Atmos. Chem. Phys.*, 17, 921-933,  
920 10.5194/acp-17-921-2017, 2017.
- 921 Zhou, Y., Zhao, Y., Mao, P., Zhang, Q., Zhang, J., Qiu, L., and Yang, Y.: Development  
922 of a high-resolution emission inventory and its evaluation and application  
923 through air quality modeling for Jiangsu Province, China, *Atmos. Chem. Phys.*,  
924 17, 211-233, 10.5194/acp-17-211-2017, 2017.
- 925 ZJBS (Zhejiang Bureau of Statistics): Statistical Yearbook of Zhejiang, China  
926 Statistics Press, Beijing, 2016 (in Chinese).



## 927 **Figure captions**

928 Figure 1. The modeling domain and the locations of the concerned provinces and their  
929 capital cities. The numbers 1-4 represent the cities of Nanjing, Hefei, Shanghai and  
930 Hangzhou, respectively. The map data provided by Resource and Environment Data  
931 Cloud Platform are freely available for academic use  
932 (<http://www.resdc.cn/data.aspx?DATAID=201>), © Institute of Geographic Sciences &  
933 Natural Resources Research, Chinese Academy of Sciences.

934 Figure 2. The spatial distributions of the simulated monthly  $\text{SO}_2$ ,  $\text{NO}_2$ ,  $\text{O}_3$  and  $\text{PM}_{2.5}$   
935 concentrations for Case 2 in D2 (unit:  $\mu\text{g}/\text{m}^3$ ).

936 Figure 3. The spatial distributions of the relative changes (%) in the simulated  
937 monthly  $\text{SO}_2$ ,  $\text{NO}_2$ ,  $\text{O}_3$  and  $\text{PM}_{2.5}$  concentrations between Cases 2 and 3 (Case 2-Case  
938 3) in D2.

939 Figure 4. The spatial distributions of the relative changes (%) in the simulated  
940 monthly  $\text{SO}_2$ ,  $\text{NO}_2$ ,  $\text{O}_3$  and  $\text{PM}_{2.5}$  concentrations between Cases 2 and 4 (Case 2-Case  
941 4) in D2.

942 Figure 5. The spatial distributions of the annual  $\text{PM}_{2.5}$  concentrations (average of  
943 January, April, July and October) for Case 2 (a) and the reduced annual  $\text{PM}_{2.5}$   
944 concentrations for Cases 3 (b) and 4 (c) in the YRD region (unit:  $\mu\text{g}/\text{m}^3$ ). Note the  
945 different color ranges in the panels for easier visualization.

946 Figure 6. The population fractions exposed to different levels of  $\text{PM}_{2.5}$  in the YRD  
947 region for Cases 2 (a), 3 (b), and 4 (c).

948 Figure 7. The spatial distributions of the mortality (a) and YLL (b) attributable to  
949  $\text{PM}_{2.5}$  exposure in Case 2 at a horizontal resolution of 9 km.

950 Figure 8. Comparisons of the estimated mortality attributable to  $\text{PM}_{2.5}$  exposure in  
951 various studies for the YRD region.

952 Figure 9. The spatial distributions of the avoided deaths and YLL attributable to the  
953 reduced  $\text{PM}_{2.5}$  exposure with ultra-low emission policy implementation at a horizontal  
954 resolution of 9 km. Note the different color ranges in the panels for easier  
955 visualization.



## Tables

**Table 1 Descriptions of the emission cases.**

Case	Description
Case 1	The emissions of coal-fired power sector were estimated based on the emission factor method without CEMS data incorporated.
Case 2	The emissions of coal-fired power sector were estimated based on the improved method by Y. Zhang et al. (2019), with CEMS data incorporated.
Case 3	All the coal-fired power plants in the YRD region were assumed to meet the requirement of the ultra-low emission policy.
Case 4	All the coal-fired power and industrial boilers in the YRD region were assumed to meet the requirement of the ultra-low emission policy.
Case 5	The emissions of all coal-fired power plants were set at zero.



**Table 2 Comparisons of the observed and simulated monthly SO<sub>2</sub>, NO<sub>2</sub>, O<sub>3</sub> and PM<sub>2.5</sub> concentrations in Cases 1 and 2 in the YRD region.**

Pollutant	R		NMB (%)		NME (%)		
	Case 1	Case 2	Case 1	Case 2	Case 1	Case 2	
SO <sub>2</sub>	Jan	0.72	0.89↑	11.44	0.52↑**	26.83	24.22↑
	Apr	0.36	0.45↑	-18.45	-22.62	31.65	34.81
	Jul	0.17	0.14	36.84	15.72↑***	58.69	48.44↑
	Oct	0.59	0.57	14.59	1.15↑***	32.49	29.22↑*
NO <sub>2</sub>	Jan	0.72	0.73↑	42.74	34.92↑*	44.25	37.88↑
	Apr	0.64	0.69↑	69.24	48.72↑***	70.24	51.81↑**
	Jul	0.71	0.71	145.42	131.65↑*	145.42	131.65↑*
	Oct	0.70	0.69	58.15	47.73↑*	58.86	49.41↑*
O <sub>3</sub>	Jan	0.74	0.75↑	-16.90	-6.40↑**	30.53	28.60↑
	Apr	0.78	0.67	-14.88	-9.89↑	23.14	27.48
	Jul	0.78	0.79↑	-34.49	-28.46↑	37.11	32.77↑
	Oct	0.80	0.78	-30.37	-28.28↑	34.32	33.60↑
PM <sub>2.5</sub>	Jan	0.89	0.90↑	-0.28	1.63	16.27	15.21↑
	Apr	0.76	0.76	9.94	2.57↑**	21.30	19.26↑
	Jul	0.64	0.63	30.44	24.08↑***	37.66	34.29↑*
	Oct	0.75	0.75	5.40	-11.80	23.34	22.28

Note: The arrow represents that the simulation results in Case 2 were improved compared to Case 1. \*, \*\*, and \*\*\* indicate the improvements are statistically significant with confidence levels of 90%, 95%, and 99 %, respectively. The R, NMB and NME were calculated using the following equations ( $P$ ,  $O$ ,  $\bar{P}$ , and  $\bar{O}$  represent the simulation, observation, averaged simulation and averaged observation values, respectively):

$$NMB = \frac{\sum_{i=1}^n (P_i - O_i)}{\sum_{i=1}^n O_i} \times 100\% \quad ; \quad NME = \frac{\sum_{i=1}^n |P_i - O_i|}{\sum_{i=1}^n O_i} \times 100\% \quad ;$$

$$R = \frac{\sum_{i=1}^n (P_i - \bar{P})(O_i - \bar{O})}{\sqrt{\sum_{i=1}^n (P_i - \bar{P})^2 \sum_{i=1}^n (O_i - \bar{O})^2}}$$



**Table 3** The relative (%) and absolute changes ( $\mu\text{g}/\text{m}^3$ , in parentheses) of the simulated monthly pollutant concentrations in different cases relative to Case 2 in the YRD region.

Pollutant	(Case 3 - Case 2) / Case 2				(Case 4 - Case 2) / Case 2				(Case 5 - Case 2) / Case 2			
	Jan	Apr	Jul	Oct	Jan	Apr	Jul	Oct	Jan	Apr	Jul	Oct
SO <sub>2</sub>	-2.7	-4.8	-6.1	-4.3	-32.9	-57.3	-64.1	-55.1	-4.3	-11.4	-12.1	-12.1
	(-0.2)	(-0.2)	(-0.1)	(-0.2)	(-2.0)	(-1.8)	(-1.5)	(-2.4)	(-0.3)	(-0.4)	(-0.3)	(-0.5)
NO <sub>2</sub>	-2.0	-2.9	-2.0	-2.5	-16.4	-21.9	-17.1	-22.8	-2.6	-5.9	-4.1	-6.2
	(-0.4)	(-0.4)	(-0.3)	(-0.4)	(-3.2)	(-3.0)	(-2.5)	(-3.7)	(-0.5)	(-0.8)	(-0.6)	(-1.0)
O <sub>3</sub>	1.7	2.2	0.8	2.2	10.4	9.7	2.6	14.0	-2.0	2.7	-1.6	4.5
	(0.4)	(0.9)	(0.3)	(0.8)	(2.6)	(4.1)	(0.8)	(4.8)	(-0.5)	(1.2)	(-0.5)	(1.5)
PM <sub>2.5</sub>	-0.1	-0.5	-1.3	-0.5	-6.2	-14.6	-21.6	-14.3	-1.7	-2.4	-4.3	-0.9
	(-0.1)	(-0.2)	(-0.4)	(-0.2)	(-4.6)	(-6.0)	(-6.5)	(-6.3)	(-1.3)	(-1.0)	(-1.3)	(-0.4)



**Table 4** The estimated mortality and YLL attributable to  $PM_{2.5}$  exposures in Case 2 over the YRD region.

	STK	IHD	COPD	LC	LRI	Total
Deaths ( $\times 10^3$ person)						
Anhui	19.6 (10.7-29.0)	19.1 (11.0-29.8)	15.2 (9.8-21.0)	8.0 (5.5-10.3)	3.1 (2.4-3.8)	65.0 (39.4-93.9)
Shanghai	4.3 (2.3-6.5)	4.2 (2.4-6.6)	4.4 (2.7-6.1)	2.6 (1.7-3.3)	0.8 (0.6-1.0)	16.3 (9.8-23.4)
Jiangsu	23.6 (12.7-35.0)	31.3 (17.8-48.8)	12.8 (8.1-17.7)	8.1 (5.5-10.5)	3.7 (2.8-4.5)	79.5 (46.8-116.5)
Zhejiang	8.7 (4.2-13.4)	6.8 (3.6-10.4)	10.8 (6.2-15.4)	5.0 (3.1-6.9)	1.6 (1.1-2.0)	32.9 (18.2-48.2)
YRD	56.2 (29.9-83.8)	61.4 (34.7-95.5)	43.3 (26.8-60.2)	23.6 (15.8-31.0)	9.2 (7.0-11.3)	193.8 (114.2-281.9)
YLL ( $\times 10^4$ year)						
Anhui	30.1 (16.6-44.0)	29.6 (17.3-45.6)	66.0 (42.3-91.1)	34.5 (23.7-44.4)	13.6 (10.4-16.4)	173.7 (110.3-241.5)
Shanghai	6.7 (3.6-9.8)	6.5 (3.8-10.0)	19.0 (11.9-26.2)	11.0 (7.4-14.4)	3.5 (2.7-4.3)	46.7 (29.4-64.8)
Jiangsu	36.2 (19.7-53.1)	48.6 (28.0-74.7)	55.6 (35.0-76.7)	35.0 (23.6-45.6)	16.0 (12.3-19.4)	191.4 (118.5-269.5)
Zhejiang	13.3 (6.5-20.5)	10.6 (5.7-16.0)	46.9 (26.7-66.6)	21.8 (13.6-30.0)	6.8 (4.8-8.9)	99.4 (57.2-141.9)
YRD	86.3 (46.3-127.4)	95.3 (54.7-146.4)	187.4 (115.9-260.6)	102.3 (68.3-134.4)	40.0 (30.1-48.9)	511.3 (315.5-717.7)



**Table 5** The reduced attributable deaths (person) and rates (in parentheses) resulting from implementation of the ultra-low emission policy in the YRD region.

	<b>STK</b>	<b>IHD</b>	<b>COPD</b>	<b>LC</b>	<b>LRI</b>	<b>Total</b>
<b>Case 3</b>						
Anhui	26 (0.13%)	19 (0.10%)	24 (0.16%)	18 (0.22%)	6 (0.18%)	92 (0.14%)
Shanghai	1 (0.03%)	1 (0.02%)	1 (0.03%)	1 (0.04%)	0 (0.04%)	5 (0.03%)
Jiangsu	51 (0.22%)	51 (0.16%)	34 (0.27%)	30 (0.37%)	11 (0.31%)	177 (0.22%)
Zhejiang	7 (0.08%)	4 (0.06%)	11 (0.10%)	7 (0.14%)	2 (0.13%)	31 (0.10%)
YRD	85 (0.15%)	74 (0.12%)	71 (0.16%)	55 (0.23%)	19 (0.21%)	305 (0.16%)
<b>Case 4</b>						
Anhui	901 (4.59%)	650 (3.41%)	848 (5.56%)	605 (7.60%)	196 (6.23%)	3200 (4.92%)
Shanghai	281 (6.46%)	204 (4.84%)	348 (7.95%)	277 (10.86%)	75 (9.20%)	1185 (7.26%)
Jiangsu	1192 (5.05%)	1179 (3.76%)	794 (6.19%)	684 (8.47%)	264 (7.14%)	4114 (5.17%)
Zhejiang	475 (5.49%)	283 (4.16%)	765 (7.06%)	491 (9.77%)	138 (8.72%)	2152 (6.54%)
YRD	2848 (5.06%)	2316 (3.77%)	2755 (6.37%)	2058 (8.71%)	673 (7.28%)	10651 (5.50%)



**Table 6 The reduced cases and rates (in parentheses) of YLL resulting from implementation of the ultra-low emission policy in the YRD region.**

	STK	IHD	COPD	LC	LRI	Total
<b>Case 3</b>						
Anhui	396 (0.13%)	285 (0.10%)	1058 (0.16%)	760 (0.22%)	243 (0.18%)	2743 (0.16%)
Shanghai	17 (0.03%)	13 (0.02%)	60 (0.03%)	45 (0.04%)	13 (0.04%)	148 (0.03%)
Jiangsu	783 (0.22%)	774 (0.16%)	1480 (0.27%)	1282 (0.37%)	491 (0.31%)	4809 (0.25%)
Zhejiang	107 (0.08%)	66 (0.06%)	483 (0.10%)	301 (0.14%)	87 (0.13%)	1044 (0.11%)
YRD	1303 (0.15%)	1138 (0.12%)	3118 (0.16%)	2388 (0.23%)	834 (0.21%)	8744 (0.17%)
<b>Case 4</b>						
Anhui	13733 (4.56%)	9946 (3.36%)	36709 (5.56%)	26218 (7.60%)	8480 (6.23%)	95086 (5.47%)
Shanghai	4284 (6.43%)	3127 (4.78%)	15083 (7.95%)	11993 (10.86%)	3233 (9.20%)	37719 (8.07%)
Jiangsu	18192 (5.02%)	18066 (3.72%)	34393 (6.19%)	29638 (8.47%)	11451 (7.14%)	111740 (5.84%)
Zhejiang	7297 (5.49%)	4380 (4.13%)	33115 (7.06%)	21255 (9.77%)	5972 (8.72%)	72018 (7.25%)
YRD	43506 (5.04%)	35518 (3.73%)	119300 (6.37%)	89104 (8.71%)	29135 (7.28%)	316562 (6.19%)



Figure 1

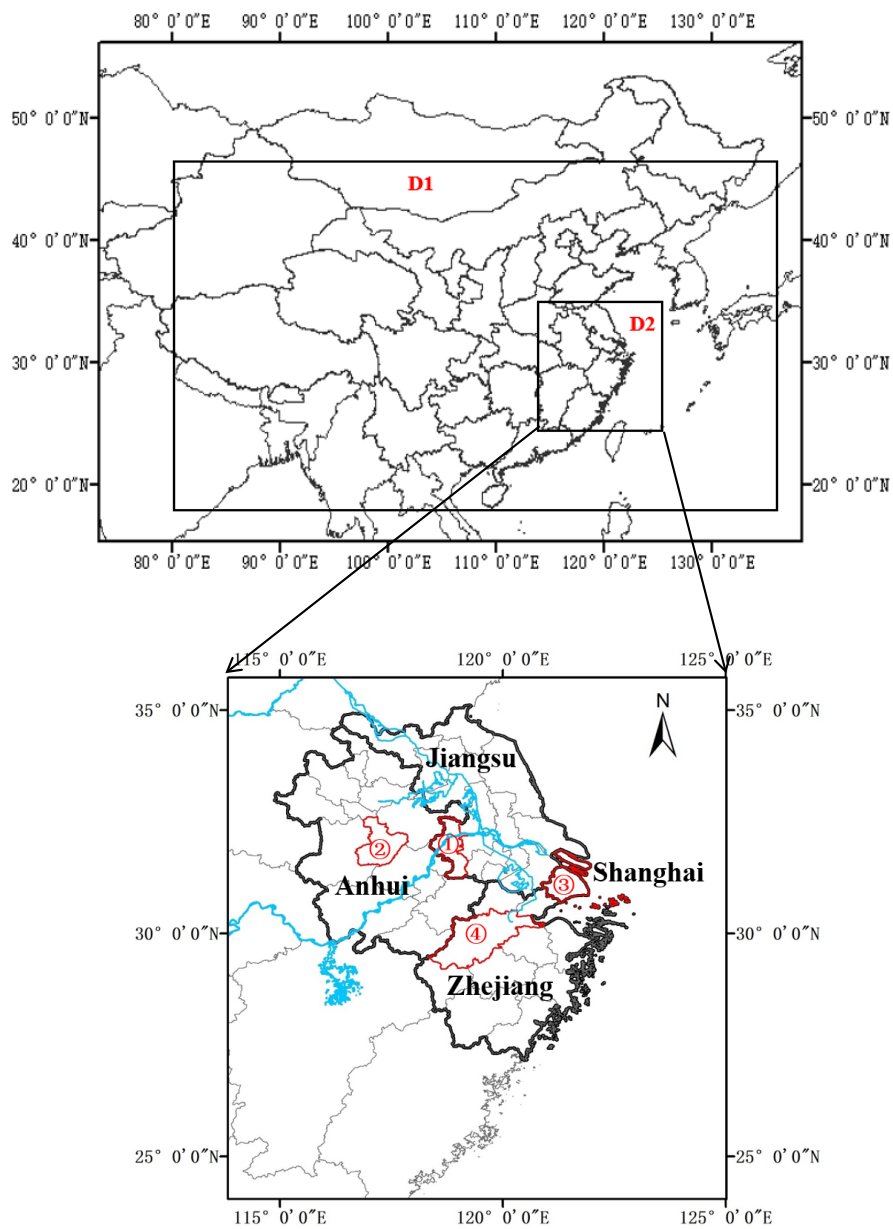


Figure 2

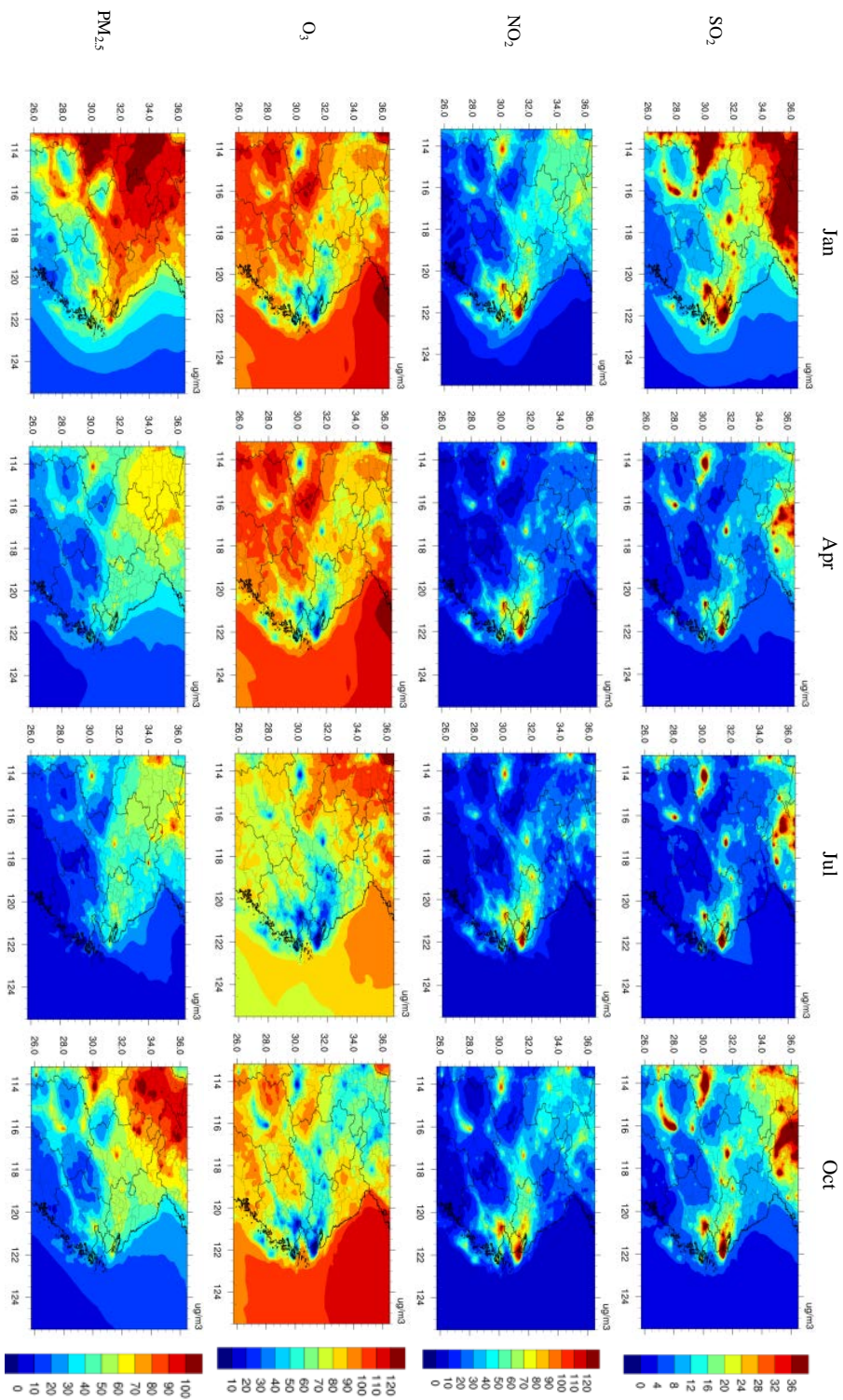


Figure 3

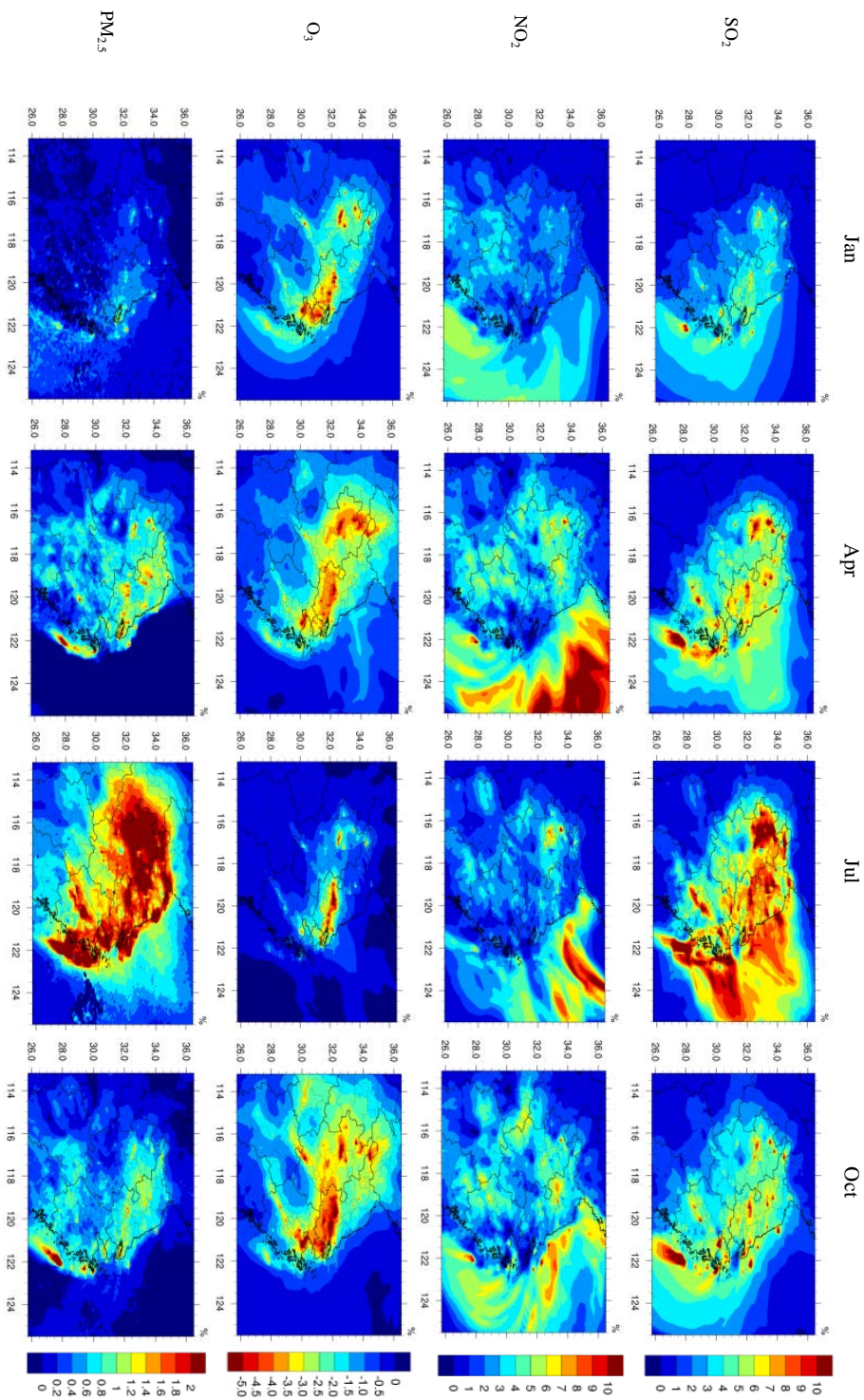




Figure 4

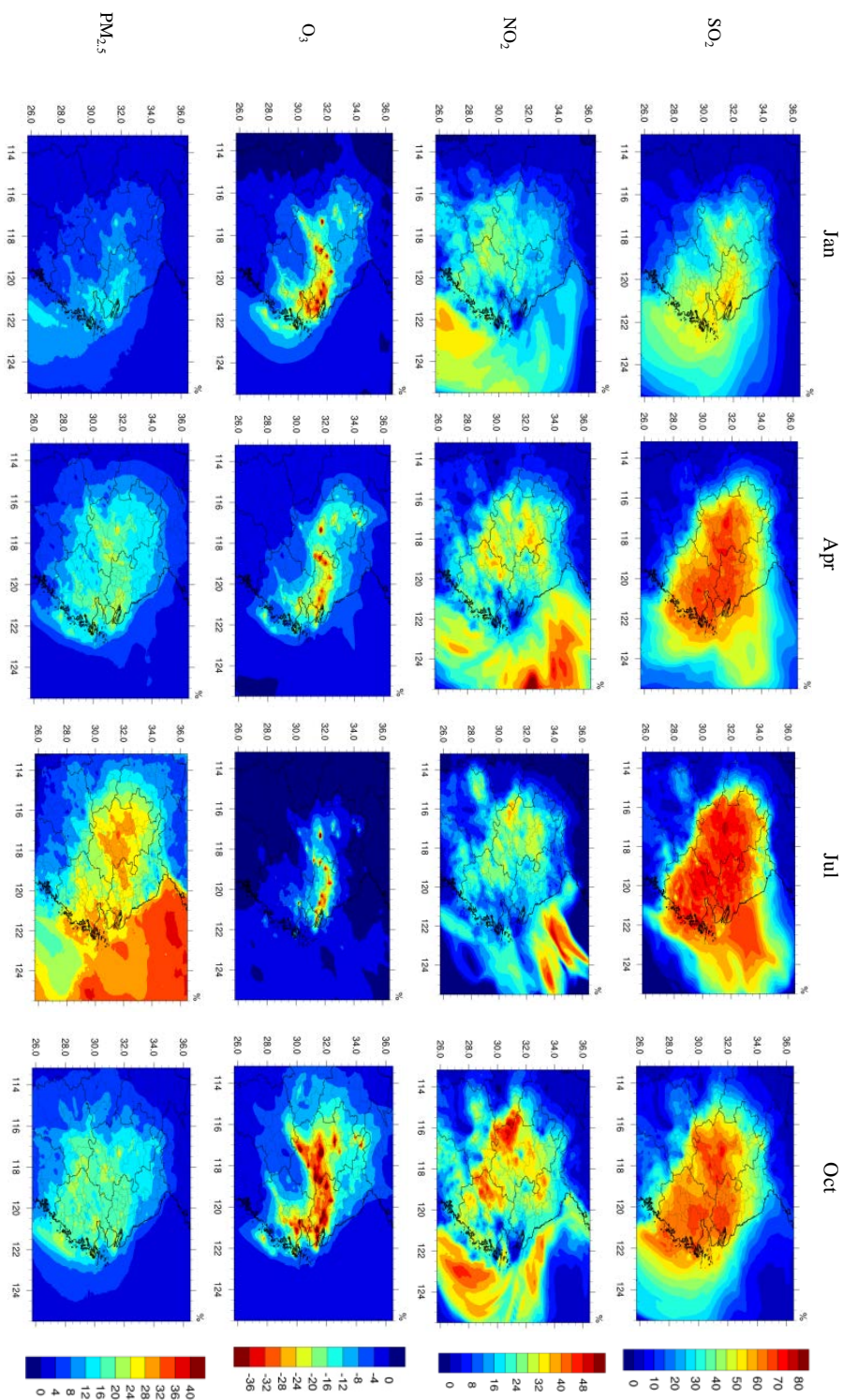




Figure 5

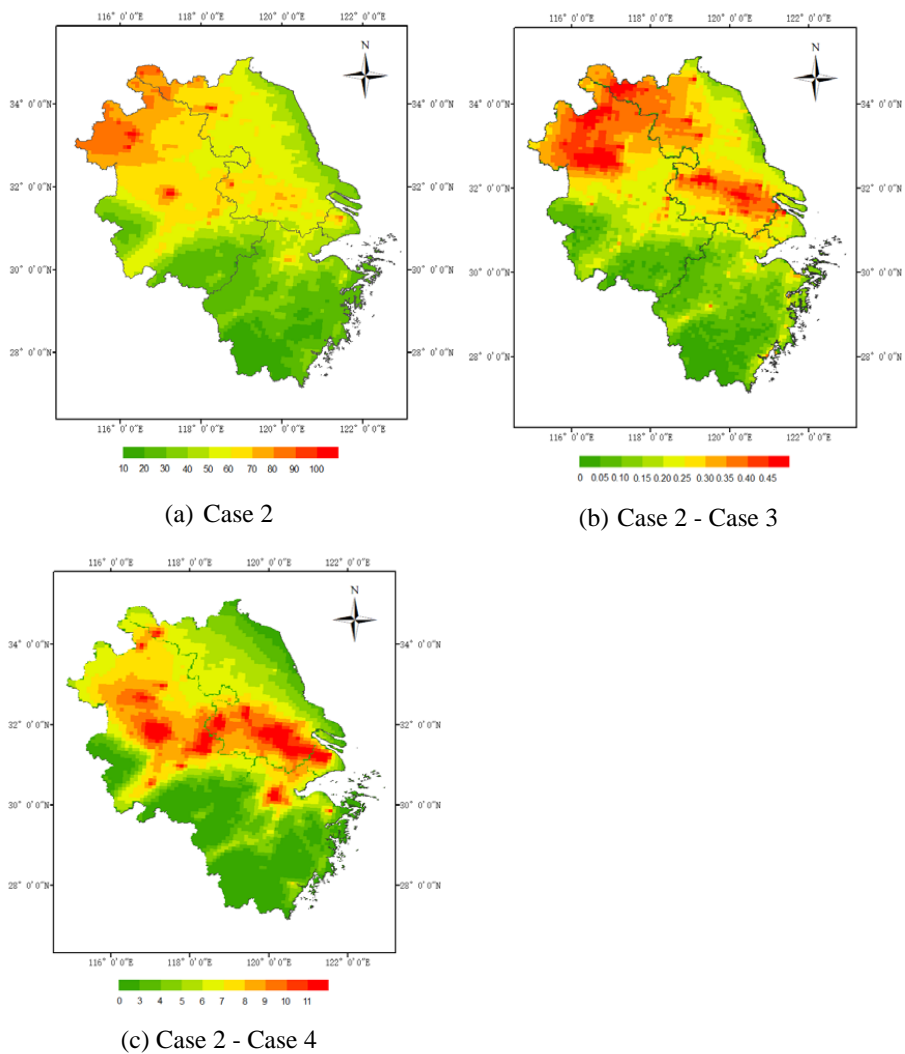
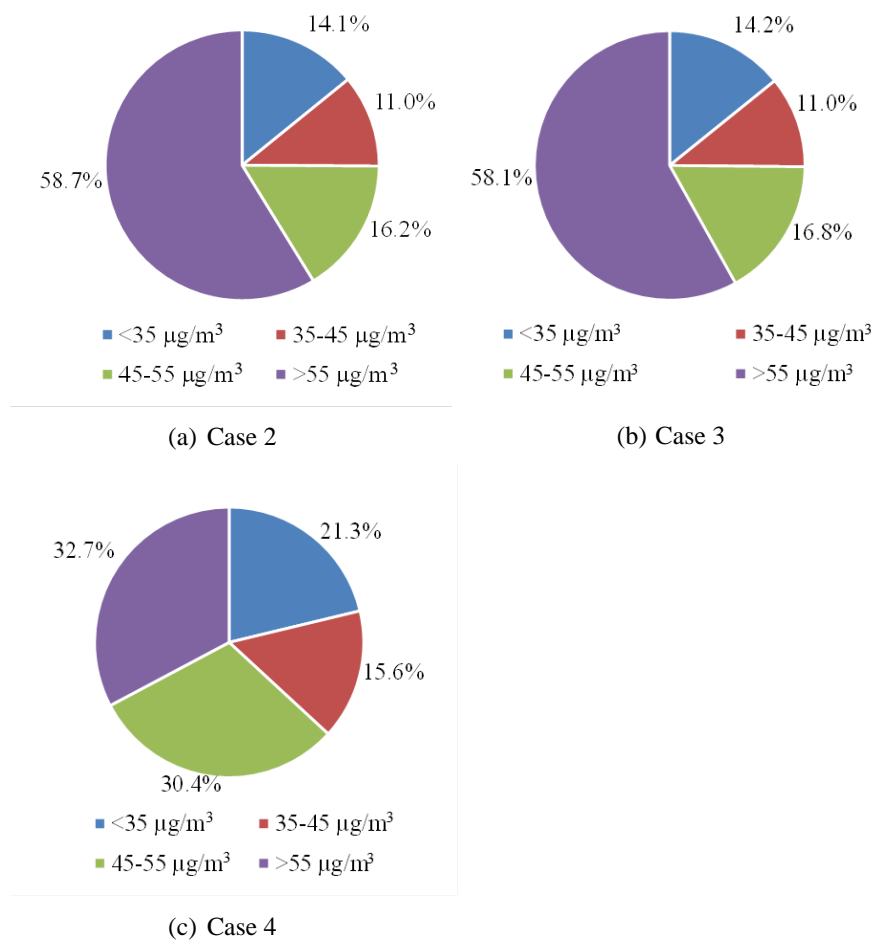


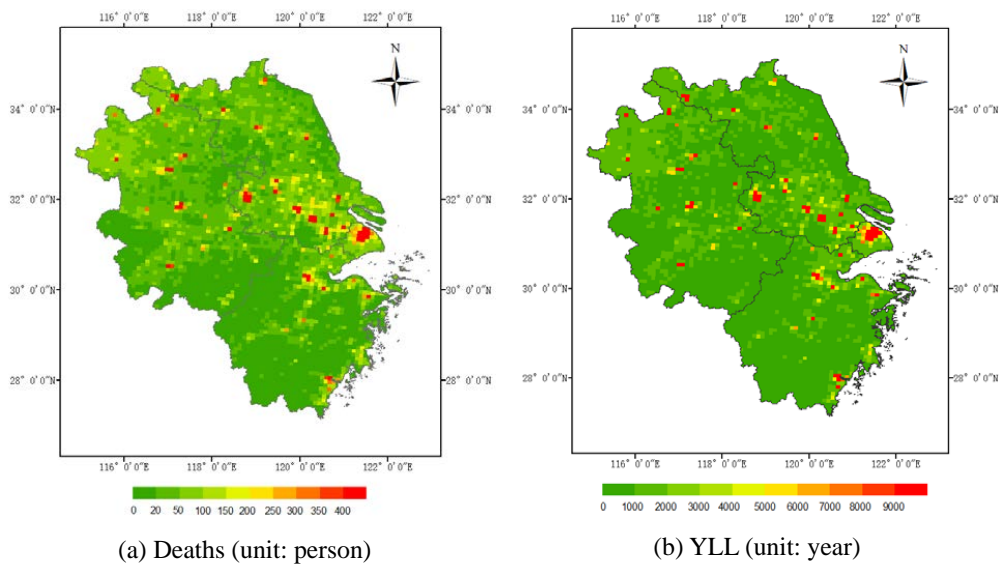


Figure 6





**Figure 7**





**Figure 8**

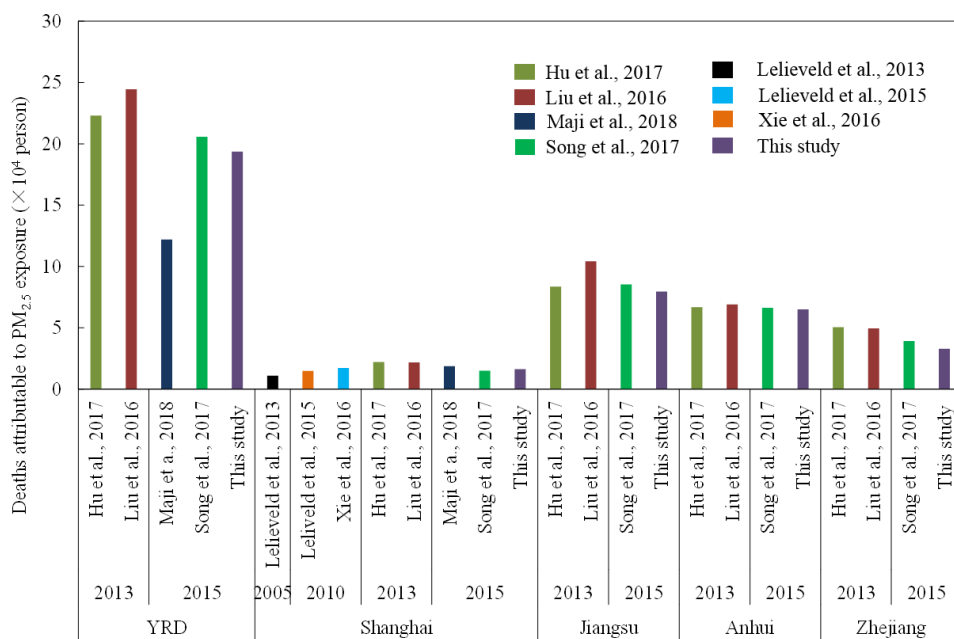




Figure 9

